



Cite this: *Mater. Horiz.*, 2020, 7, 2237

Received 13th May 2020,  
Accepted 22nd June 2020

DOI: 10.1039/d0mh00798f

rsc.li/materials-horizons

## Lignin-based smart materials: a roadmap to processing and synthesis for current and future applications

Adrian Moreno and Mika H. Sipponen \*

Biomass-derived materials are green alternatives to synthetic plastics and other fossil-based materials. Lignin, an aromatic plant polymer, is one of the most appealing renewable material precursors for smart materials capable of responding to different stimuli. Here we review lignin-based smart materials, a research field that has seen a rapid growth during the last five years. We describe the main processing and chemical synthesis routes available for the fabrication of lignin-based smart materials, and focus on their use as sensors, biomedical systems, and shape-programmable materials. In addition to benchmarking their performance to the state of the art fossil counterparts, we identify challenges and future opportunities for the development of lignin-based smart materials towards new high-performance applications.

### 1. Introduction

The development of materials from renewable resources *via* sustainable methodologies is one of the most promising solutions to reduce exploitation of fossil resources that is linked to increasing greenhouse gas emissions and climate change.<sup>1,2</sup> In addition to synthetic polymers of renewable origin such as poly(lactide) (PLA), poly( $\epsilon$ -caprolactone) and poly(3-hydroxybutyrate) (PHB),<sup>3–5</sup>

Department of Materials and Environmental Chemistry, Stockholm University, SE-10691, Stockholm, Sweden. E-mail: [mika.sipponen@mmk.su.se](mailto:mika.sipponen@mmk.su.se)



Adrian Moreno

holds a Postdoctoral Fellow position in the Sustainable Materials Chemistry (SUSMATCH) group at Stockholm University with Assist. Prof. Mika H. Sipponen. His research interests lie in the development of novel lignin-based functional materials.

Adrian Moreno received his BSc and MSc in chemistry from the Universitat Rovira i Virgili (Spain). He obtained his PhD in 2019 working on Single Electron Transfer-Living Radical Polymerization (SET-LRP) and the design of stimuli-responsive polymers under the supervision of Prof. Gerard Lligadas and Prof. Marina Galia. During his PhD, he did an exchange in the group of Prof. Virgil Percec (University of Pennsylvania, USA). Currently, he

abundant and renewable plant biomass and its natural polymeric components are attractive material precursors.<sup>6,7</sup> Next to cellulose, which is the most important natural polymer and constituent of plant biomass, lignin has been considered “the black sheep” and a low-value byproduct that is mostly combusted in lignocellulosic biorefineries and chemical pulping processes.<sup>8–10</sup> This disdain over lignin is not warranted based on its natural functions such as adding strength and rigidity to the plant cells walls, enabling transport of water, and protecting from pathogens and insects.<sup>11,12</sup>

Lignin is synthetized mainly from *p*-coumaryl alcohol, coniferyl alcohol, and sinapyl alcohol monomers (Fig. 1a) *via*



Mika H. Sipponen

Chemistry in the Department of Materials and Environmental Chemistry at Stockholm University. His Sustainable Materials Chemistry (SUSMATCH) group develops novel lignin-based processes and materials following the principles of green chemistry.



an enzyme-initiated dehydrogenation, radical coupling, and dimerization reactions, resulting in an amorphous and three-dimensional (3D) material with both ether and carbon–carbon bonds.<sup>13,14</sup> It is impossible to give an exact molecular structure of lignin because various different isolation processes cause structural changes and insertion of new functional groups. Furthermore, lignins are usually referred to as polymers, but isolated technical lignins can also be viewed as mixtures of oligomers. For instance, lignin obtained from the kraft pulping process has an average degree of polymerization of 30 compared to a DP of about 6000 of a polystyrene.

In recent years, there have been widespread efforts to upgrade lignin towards advanced engineered materials.<sup>15</sup> In fact, lignin is an aromatic biopolymer gifted with numerous attractive properties such as high (>60 atom%) carbon content, high thermal stability, biodegradability, antioxidant activity, absorbance of UV irradiation, and antimicrobial activity.<sup>16–19</sup> Beyond conventional bulk and low-cost materials such as concrete plasticizers,<sup>20–22</sup> the development of lignin-based smart materials is now emerging as the next generation of value-added applications. This new class of smart materials has the ability to convert specific stimuli to defined outputs and change or activate a functional property of the material (Fig. 1b). It has become important to provide control over these stimuli-responsive properties, and this often requires modification or insertion of new functional groups capable of changing one of their properties in a spatio-temporal fashion in response to external stimuli such as temperature, pH, light or electricity among others.

There are several excellent reviews dedicated to the synthesis and applications of lignin-based materials<sup>23–31</sup> but none of these have identified lignin-based smart materials as an emerging research field. Therefore, in this review we visit the recently published literature on the synthesis and applications of lignin-based smart materials, and make a critical comparison to the state of the art benchmark materials prepared largely from fossil-based precursors. We begin with a brief roadmap to different chemical and processing routes and continue with an analysis of lignin-based smart materials for (1) sensing and biosensing, (2) controlled encapsulation and release, especially in biomedical systems, and (3) shape memory

programmable materials. Finally, we conclude with challenges and perspectives for these advanced materials in current and future applications.

## 2. Roadmap to lignin-based smart materials

There are many different routes to obtain lignin polymers, oligomers, and dimers/monomers from plant biomass and their conversion to smart materials (Fig. 2). Low molecular weight phenolic molecules can be produced from lignin by cleavage of inter-unit linkages, among which aryl ether linkages ( $\beta$ -O-4') typically account more than 50% of bonds formed during the polymerization process. Other relevant linkages include resinol ( $\beta$ - $\beta$ ), phenylcoumaran ( $\beta$ -5'), biphenyl (5-5'), diphenyl ether (4-O-5') and diphenyl methane ( $\beta$ -1), which are significantly more complicated to degrade.<sup>32</sup> The chemical structure of lignin is strongly related to its botanical origin and the isolation process, and recent progress in different analytical techniques have made analysis of the chemical bonds a less daunting task.<sup>33,34</sup>

The pulp and paper industry is the primary source of technical lignin. As reviewed elsewhere,<sup>35,36</sup> lignin is dismantled from cellulosic fibers by thermochemical treatments, resulting in depolymerization and solubilization of lignin, while at the same time non-native “condensed” bonds are formed at the reactive sites. The most relevant technical lignins for material applications are lignosulfonates (LS), kraft lignin (KL), organosolv lignin (OSL) and soda lignin (SL).<sup>37–39</sup> It is important to mention that the selection of the type of lignin is strongly related to the desired application. For instance, less pure preparations might be readily accessible to lignin-derived plastics<sup>40,41</sup> or composites,<sup>21,22,30</sup> whereas highly purified or fractionated lignins should be considered for high-performance materials such as biomedical applications.<sup>42,43</sup>

The most straightforward way is to use crude technical lignins to enhance properties of existing polymeric materials.<sup>44,45</sup> For instance, lignin has been used as an antioxidant and UV-shielding additive in plastics,<sup>46,47</sup> and stabilizer and flame retardant

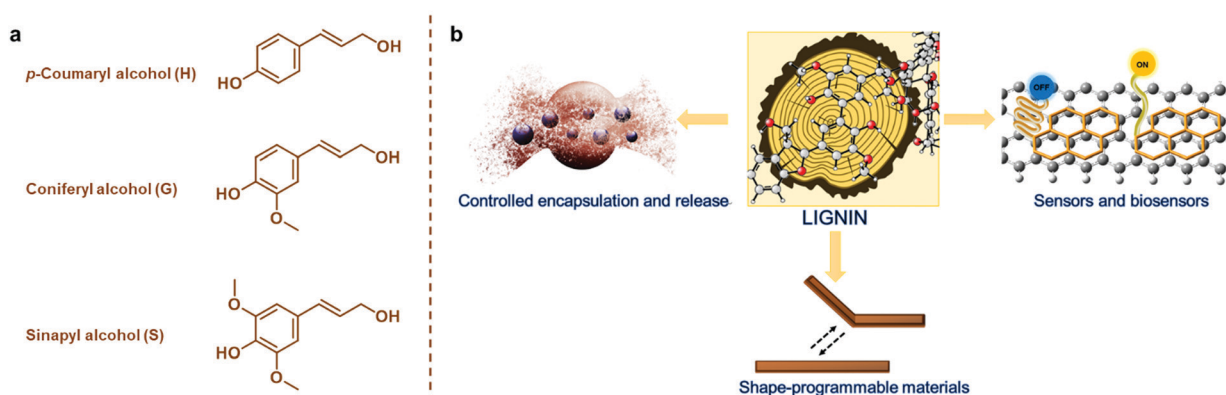


Fig. 1 (a) Monomeric precursors of lignin. (b) An overview of lignin-based smart materials covered in the present review.



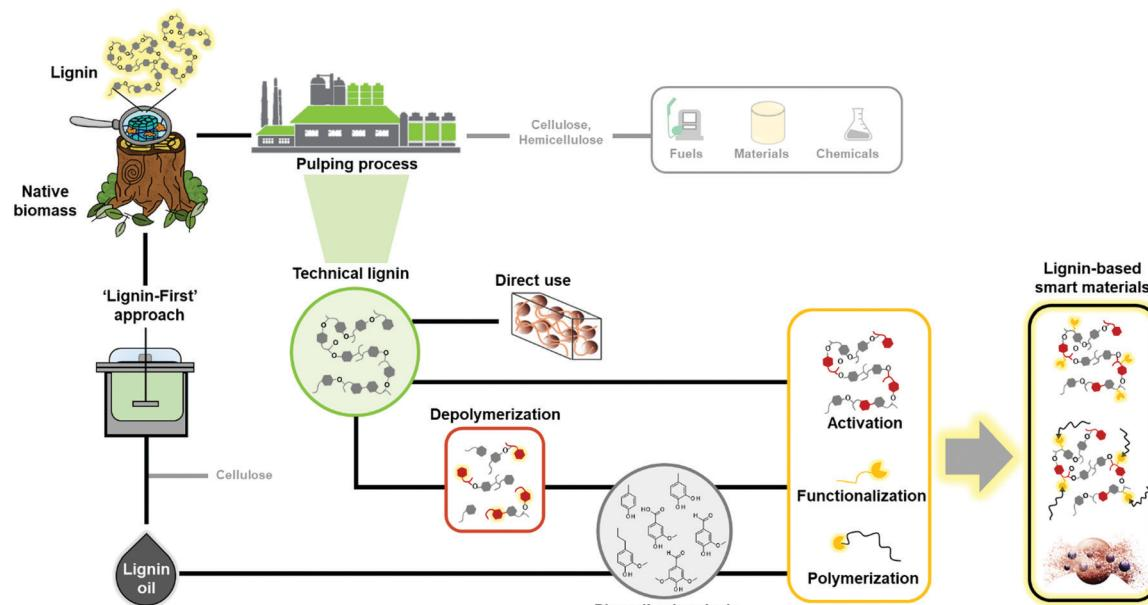


Fig. 2 Roadmap from native lignocellulosic biomass to lignin-based smart materials.

agent in fillers.<sup>48,49</sup> However, in most of these applications only a minor amount of lignin can be blended due to its inferior mechanical properties and low compatibility with many polymers.<sup>25</sup> Chemical modification of lignin has been postulated as the main alternative to improve its material properties for polymers. These processes increase the reactivity of lignin by targeting its functional groups such as hydroxyl, methoxyl, carbonyl, or carboxyl groups through chemical modification processes such as hydroxalkylation, esterification, and amination, among others (Fig. 3a).<sup>23,26,50–58</sup> Many of these chemical

modifications have attempted to convert lignin macromolecules into macromonomers and subsequently graft classical monomers or polymers, and in this way, synthesize lignin-based functional polymers.<sup>23,26,28</sup>

Well-defined lignin graft copolymers can be elaborated by two main methodologies: “grafting from” and “grafting to” (Fig. 3b). In the “grafting from” technique, lignin is used as a macromonomer and usually monomers react with functional groups on lignin (e.g. hydroxyl groups or alkyl halide esters) in a way that the growing polymer chain is assembled on the lignin core.

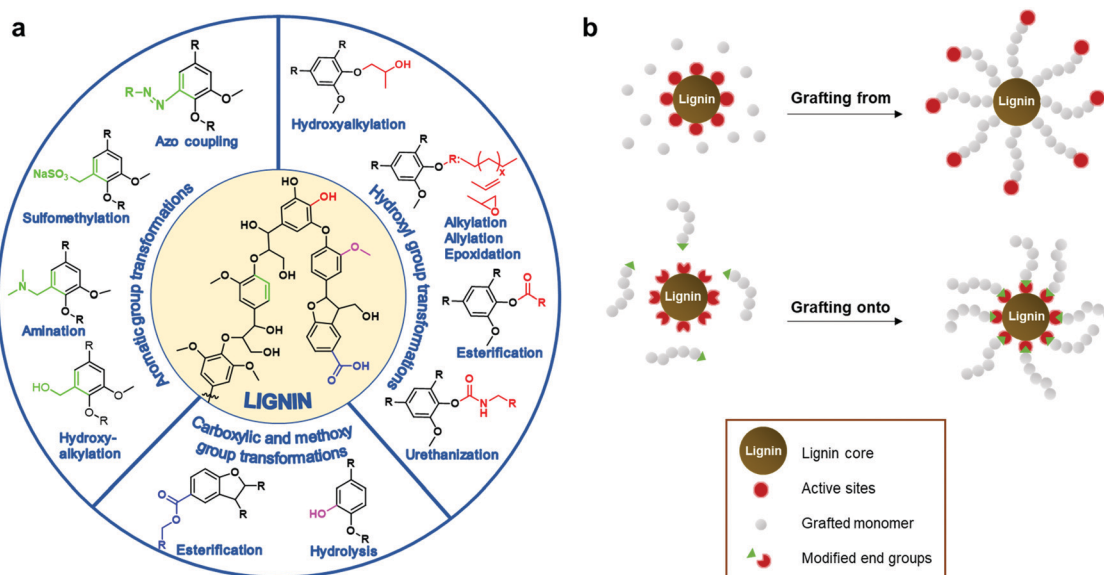


Fig. 3 (a) Summary of chemical transformation commonly employed to increase the chemical functionality of lignin. (b) General strategies to synthesize lignin-based graft polymers.



Among the different “grafting from” polymerizations, atom transfer radical polymerization (ATRP) and ring opening polymerization (ROP) have been considered the most powerful methodologies to synthesize, in a controlled manner, well defined lignin-based polymers for multiple applications ranging from biobased composites to gene delivery systems.<sup>59–62</sup> In the case of the “grafting to” technique, a previously synthesized polymer chain is anchored to the lignin core through a functional chain end group which serves as a reactive point towards lignin.<sup>23,63–66</sup> This technique presents some advantages such as the ability to tune the length of the grafted chains prior to the grafting step and the possibility to conduct a complete characterization prior to the grafting step. Among the different reactions to perform the coupling between lignin and the synthesized polymer chain, “click” chemistry reactions, as is the case of Cu(i)-catalyzed azide–alkyne cycloaddition (CuAAC), have emerged as the preferred option due to the formation of the desired lignin copolymers in a simple and quantitative way.<sup>67,68</sup>

The recent years have revealed that many different types of technical lignins are suitable precursors for the synthesis of a wide range of materials.<sup>23,24,35,36,69,70</sup> In contrast, the greatest hurdle in the production of aromatic chemicals is the recalcitrance of lignin resulting from the pulping processes. To circumvent these barriers, catalytic fragmentation following so-called “lignin first” concepts have shown much greater yields and selectivity of aromatic compounds, but these processes use costly metal catalyst (e.g. Ni, Co or Rh) that are difficult to recycle from the heterogeneous reaction mixtures.<sup>71–73</sup> The resulting lignin oil fraction is enriched in low molecular weight aromatic monomers and dimers. The use of heteroatom-containing reagents for the cleavage of lignin was recently reviewed.<sup>74</sup> This approach offers the possibility to generate lignin-derived heteroatom-containing compounds of interest to many applications such as pharmaceutical precursors (e.g. aniline) or hydrogen storage materials (e.g. lithium phenolates and phenoxides). Other common routes to obtain aromatic chemicals from lignin is through fragmentation or depolymerization processes, which involve pyrolysis, oxidation, hydrogenation, gasification, and microbial conversion.<sup>16,75–77</sup> These low molar mass compounds include phenol, vanillin, guaiacol, *p*-cresol, and catechols among others, many of which are useful starting chemicals for the design and synthesis of novel biobased polymers for different applications, through different polymerization routes including polycondensation,<sup>78,79</sup> acyclic diene metathesis (ADMET),<sup>80</sup> and controlled radical polymerization techniques.<sup>81,82</sup> Nevertheless, it is important to keep in mind that while a wide range of aromatic chemical products can be obtained from lignin, to date only vanillin is produced on a commercial scale (17,000 ton per year) *via* an alkaline oxidation method.<sup>83</sup>

Regardless of the molecular weight or source of lignin, chemical modification is an inevitable step to smart materials. One of the routes is to activate or functionalize isolated lignin or its fractions to generate responsive molecules for smart materials (Fig. 2). Another, hitherto less studied approach is to functionalize lignin-derived monomers and use them to synthesize polymers or to modify technical lignins of higher

molecular weight. The latter example comes with an added benefit of lower environmental penalty compared to the sole use of petroleum-based chemicals as sources of reactive groups. However, the chemical functionalities offered by non-functionalized lignin are limited in terms of polymerization or grafting sites.

### 3. Applications and materials chemistry of lignin-based smart materials

Lignin-based smart materials possess the ability to sense external stimuli and translate it into an observable response based on physiochemical changes.<sup>27</sup> A wide range of different stimuli are available such as pH, temperature, mechanical force or electric field and their development is usually motivated and driven by inspiration from nature.<sup>84,85</sup> The following sections are dedicated to the recent developments of lignin in smart materials and their selected applications.

#### 3.1 Sensor and biosensing applications

Sensors are an important class of self-integrated devices with the ability to receive specific inputs from a surrounding media and translate them into output signals that can be transformed into a readable result. A biosensor is a device designed to be able to detect biological species of interest even in the presence of other interfering species. Likewise, lignin-based sensors have attracted considerable attention due to their ability to detect and generate quantifiable signals from complex mixtures (Table 1).

**3.1.1 Lignin-based carbon and graphene quantum dots for sensing applications.** Lignin-based carbon quantum dots (LCQDs) have emerged as a new class of materials in applications such as metal ion sensors, bio-imaging and biosensors.<sup>43,86–91</sup> Most of the sensors formulated on LCQDs work based on the quenching or the prevention of the quenching of fluorescence emission in the presence of certain analytes such as a metal ions.<sup>92</sup> Among the different quenching mechanisms, LCQDs work basically by static quenching pathways, where the interaction of LCQDs and a quencher (analyte) lead to the formation of a nonfluorescent ground-state complex, which alters the absorption spectrum of LCQDs, generating a quantifiable response.<sup>91</sup>

LCQDs are characterized by a low cytotoxicity and a good biocompatibility, but perhaps one of the most appealing features is their low cost-production from non-food resources and relative easy manufacturing process in comparison to carbon quantum dots (CQDs) based on precursors such as citric acid,<sup>93,94</sup> gelatins<sup>95</sup> and chitosan<sup>96,97</sup> among others,<sup>98,99</sup> which generally require more complex reaction conditions than LCQDs.

Chen *et al.* were the first to report the synthesis of LCQDs *via* hydrothermal processes using hydrogen peroxide ( $H_2O_2$ ) as an oxidizing agent.<sup>86</sup> However, these early LCQDs were irregular and weakly luminescent when used for biological labeling of tumorous cells (HeLa cell line). Later, LCQDs with potential



Table 1 Summary of lignin-based smart materials for sensing applications

Type of sensor	Type of lignin material	Field of application	Ref.
Biosensor	LCQDs	Bioimaging and biological labelling	43, 86, 88 and 90
Biosensor	LCQDs	Drug release and bioimaging	87
Chemical sensor	LCQDs	Fe <sup>3+</sup> detection and bioimaging	89
Chemical sensor	LCQDs	Metal-ion detection and bioimaging	91
Chemical sensor	LGQDs	Detection of H <sub>2</sub> O <sub>2</sub>	107
Immunosensor	Lignin/peptide-based gold electrode	Detection of antibody (Ab)	110
Biocatalytic sensor	Silica/lignin hybrid electrode	Detection of glucose	111
Biocatalytic sensor	Magnete/lignin hybrid electrode	Detection of glucose	112
Pressure sensor	Polydimethylsiloxane-lignin composite	Detection of pulse rates and muscle movement	120
Pressure sensor	Lignin-based hydrogel	Detection of pulse rates and force requirement	122
Humidity sensor	Graphene oxide-lignin composite	Detection of humidity moisture	121
Chemical sensor	Lignin-based polymeric composite	Detection of chromate ions	123 and 124
Biosensor	Lignin-rhodamine polymer	Bioimaging and biological labelling	127
Chemical sensor	Lignin-porphyrin polymer	Detection of heavy metal ions	129
Chemical sensor	Lignin nanoparticles	Detection of formaldehyde	133
Chemical sensor	Lignin-silver nanoparticles (AgLNPs)	Detection of Hg <sup>2+</sup> and Ni <sup>2+</sup>	135, 139 and 140

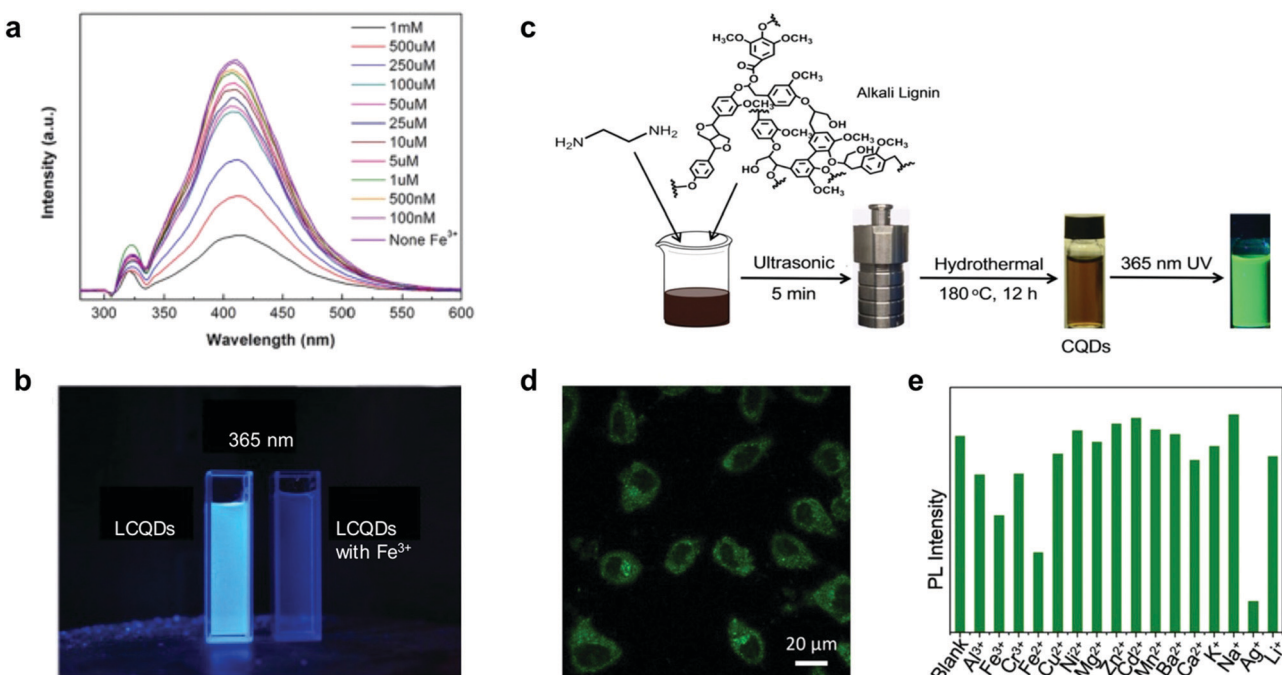


Fig. 4 Use of LCQDs for sensing applications: (a) fluorescence change of LCQD with different aqueous Fe<sup>3+</sup> concentrations. (b) LCQDs without and with Fe<sup>3+</sup> under 365 nm UV light irradiation. Adapted with permission from ref. 89. Copyright © 2019, Elsevier Ltd. (c) Schematic representation of the one-pot synthesis of LCQDs; (d) confocal fluorescence image at 488 nm excitation wavelength of LCQDs in the presence of HeLa cells; (e) sensitivity and selectivity of LCQDs for a variety of different metal ions. Adapted with permission from ref. 91. Copyright © 2019 Wiley-VCH Verlag GmbH & Co. KGaA, Weinheim.

theranostic applications were also developed by Rai *et al.* via microwave assisted depolymerization of sodium lignosulfonate followed by a carbonization process assisted by microwave irradiation.<sup>87</sup> After the synthesis, the LCQDs were reduced by sodium borohydride (NaBH<sub>4</sub>) to lignin-based carbon quantum dots (r-LCQDs). The resulting r-LCQDs showed the ability to adsorb and release curcumin as a model drug compound at neutral pH (drug loading efficiency was 67.4% and 82% of curcumin released after 72 hours), and bio-imaging studies showed that r-LCQDs could penetrate into tumorous cells (A549 and SW480 cell lines) *via* simple diffusion through the

cell membrane. This work reflects the potential of these systems for therapeutic and cancer diagnosis applications. However, the attractiveness of this approach suffers from the use of NaBH<sub>4</sub> that is an expensive, harmful and highly sensitive reducing agent. Therefore, it is important to note that greener reducing agents such as ascorbic acid or even lignin itself should be considered for future applications.<sup>29,100,101</sup>

Xue *et al.* reported the synthesis of hybrid LCQDs by one pot hydrothermal treatment of lignin with different molar ratios of citric acid and ethanediamine.<sup>88</sup> The resulting LCQDs showed promising results for bio-imaging applications. However, the



long reaction times and energy-consuming fabrication process make them less appealing from a synthetic point of view. Later, Shi *et al.* reported a facile synthesis of LCQDs by the introduction of secondary amine groups into lignin through Mannich and Michael addition reactions followed by carbonization, milling and filtration.<sup>89</sup> The resulting LCQDs showed an excellent performance for the detection of iron ions ( $\text{Fe}^{3+}$ ) in a wide range of concentrations (1–100 nM) and lower detection limits (8 nM) compared to those of other CQDs based on foodstuff precursors as is the case of citric acid (0.3  $\mu\text{M}$ )<sup>102</sup> or red lentils (0.10  $\mu\text{M}$ )<sup>103</sup> among others<sup>104,105</sup> (Fig. 4a and b). Moreover, fluorescence imaging demonstrated excellent image quality and biocompatibility of the LCQDs uptaken by biological cells.<sup>89</sup>

It is also important to point out that heteroatom doping with elements such as nitrogen or boron is a viable strategy towards increasing the quantum yields (QY) associated with high fluorescence response.<sup>88,89</sup> For instance, Ding *et al.* prepared blue fluorescent LCQDs from kraft lignin *via* a two-step process involving sonication in nitric acid followed by hydrothermal treatment.<sup>90</sup> However, the prepared LCQDs contained a large number of defects which inhibits their use in certain applications such as in bioimaging where broad absorption and high QY are required. More recently, Zhang *et al.* also reported the preparation and LCQDs with bright green fluorescence from kraft lignin by a simple one-pot method.<sup>91</sup> In this case the prepared LCQDs revealed notable luminescence properties to be applied in cell imaging applications and also as ion detection sensors, with high sensitivity towards silver ion ( $\text{Ag}^+$ ) (Fig. 4c–e), comparable to those reported previously for other CQDs based on foodstuff precursors such as broccoli.<sup>106</sup>

In a different approach, Niu *et al.* reported the use of cellulolytic enzymatic lignin (CEL) for the synthesis of LCQDs *via*  $\pi$ – $\pi$  electric interactions induced molecular aggregation using ethanol as solvent.<sup>43</sup> This methodology enables the synthesis of LCQDs without hydrothermal carbonization by the aggregation induced emission (AIE) effect. The LCQDs exhibited one- and two-photon fluorescence emission (320 and 800 nm) and biocompatibility with HeLa cells. These properties of the LCQDs together with their absorption of near-infrared (NIR) light make these materials promising for bio-imaging applications.

Synthesis of lignin-based graphene quantum dots (LGQDs) was recently demonstrated by using recyclable *ortho*-aminobenzene-sulfonic acid as solvent to prepare lignin nanoparticles (LNPs) followed by their transformation into LGQDs by hydrothermal carbonization.<sup>107</sup> The LGQDs were applied as sensitive probes for the detection  $\text{H}_2\text{O}_2$ , a common oxidant in biological systems, due to their high UV absorbance and good biocompatibility properties. The LGQDs exhibited efficient fluorescence quenching in response  $\text{H}_2\text{O}_2$  concentrations as low as 0.13 nM, representing a significant improvement compared to those reported previously for graphene QDs (0.15–3  $\mu\text{M}$ ).<sup>108,109</sup> Such a high sensitivity towards  $\text{H}_2\text{O}_2$  was rationalized later through a detailed density functional theory (DFT) study, which revealed that the sulfonyl group localized in the middle of LGQDs serves as the specific binding site towards  $\text{H}_2\text{O}_2$ .<sup>107</sup>

### 3.1.2 Lignin as a precursor for the preparation of biosensors.

Biosensor electrodes have been constructed from lignin not only because of its low cost, but also due to its relative good compatibility with some polymeric matrixes.<sup>110–112</sup> Lignin-based biosensors consist of composites incorporating biomolecules such as enzymes or non-catalytic peptides and proteins. Generally, the response of the systems is a result of the capture of the biomolecules present in biological samples (*e.g.* glucose),<sup>111</sup> which produces changes in the surrounding medium or macroscopic properties of the system such as pH, temperature or electrical conductivity that can be translated to a quantifiable response. In this context, Cerrutti *et al.* reported the fabrication of an immunosensor by depositing layer by layer (LbL) films composed of an antigenic peptide (p17-1) and lignin onto gold electrodes.<sup>110</sup> The resulting immunosensor showed a sensitivity lower than 0.1 ng  $\text{mL}^{-1}$ , however still higher compared to other reported biosensors,<sup>113–115</sup> towards the recognition of an antibody (Ab) associated with the human immunodeficiency virus (HIV). In addition, the immunosensors preserved their activity for more than two months, which is superior to many enzyme-based immunosensors, whose lifetime is normally limited to 4–6 weeks.<sup>116</sup> Later, Jędrzak *et al.* developed a biocatalytic sensor using silica/lignin hybrid material as a matrix to immobilize glucose oxidase (GOx), followed by the electrode preparation using graphite as dispersing agent and ferrocene as redox mediator (Fig. 5a and b).<sup>111</sup> The presence of lignin in the original immobilization matrix allowed a significant improvement on enzyme immobilization (25 mg  $\text{g}^{-1}$  of GOx) compared to only silica (12.88 mg  $\text{g}^{-1}$ ), which demonstrated the benefits to incorporate lignin in this material. The biosensor showed a linear response to glucose in the range of 0.5–9 mM with a detection limit of 145  $\mu\text{M}$ , comparable to those reported for other systems.<sup>117–119</sup> Moreover, the prepared biosensors also demonstrated feasibility to determine glucose in biological samples with low standard deviation values (less than 3%).<sup>111</sup> The same group reported magnetite/lignin nanoparticles as an efficient matrix to immobilize GOx and fabricate glucose biosensors with similar properties than the previously mentioned.<sup>112</sup> Aside from the integration of lignin to develop electrodes for sensor applications, lignins have also proven to be useful matrices for the design of other lignin-based composites for sensing applications, as is the case of flexible pressure sensors for wearable electronics based on lignin/polydimethylsiloxane (Fig. 5c and d),<sup>120</sup> humidity sensors based on lignin/graphene oxide<sup>121</sup> or organohydrogels as strain sensors<sup>122</sup> (Fig. 5e).

### 3.1.3 Synthesis of lignin-based nanomaterials and composites for sensing applications.

Lignin-based polymers have also attracted attention in the preparation of carbon nanotubes for sensing applications. Here, the interest in lignin lies in its rigid polyaromatic structure and the presence of different functional groups such as carboxylic acid and phenolic hydroxyl groups which can chelate cationic substances such as transition metals.<sup>123,124</sup> For instance, Faria *et al.* synthesized lignin–polyurethane copolymers doped with carbon nanotubes for the detection of chromate ions at acidic pH and with

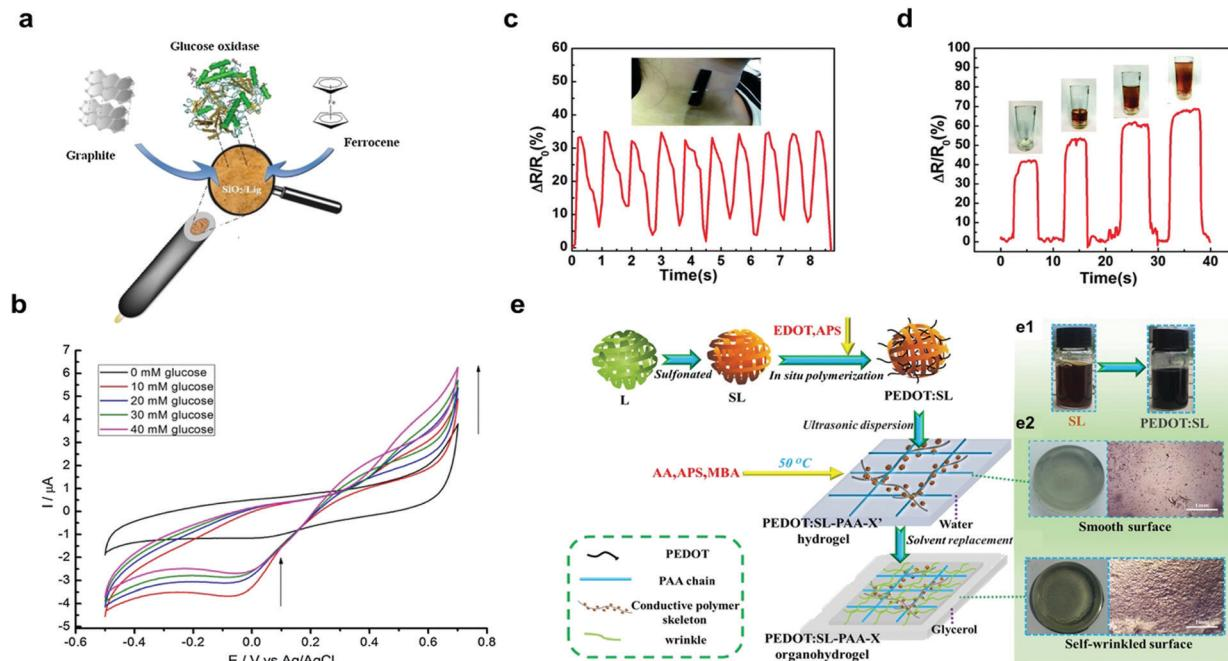


Fig. 5 Lignin-based materials as biosensors: (a) schematic representation of preparation of  $\text{SiO}_2$ –graphite–ferrocene–lignin hybrid electrode; (b) cyclic voltammetry signals of  $\text{GOx}$ – $\text{SiO}_2$ –lignin biosensor (from 10 mM to 40 mM) with an increase in oxidation current (from 0.4 V up to 0.7 V) with increasing glucose concentration. Adapted with permission from ref. 111. Copyright © 2018, Elsevier Ltd. Performance of lignin/polydimethylsiloxane composites as sensitive flexible pressure sensors: (c) measurement of arterial pulse; (d) measurement of the power required to pick up a cup. Adapted with permission from ref. 120. Copyright © 2018, Royal Society of Chemistry. Lignin-based hydrogel as a wearable sensor: (e) schematic synthesis of lignin–PEDOT based organohydrogel applied as a wearable sensor; (e1) color change of the solution during the synthesis of lignin–PEDOT based organohydrogel (e2) macro- and surface morphology of the lignin–PEDOT based organohydrogel. Adapted with permission from ref. 122. Copyright © 2019, Elsevier Ltd.

potential application as ion-selective membranes.<sup>123</sup> In the same vein, Rudnitskaya *et al.* reported lignin–poly(propylene oxide) copolymers doped with carbon nanotubes as an efficient sensor to detect chromate ions in acidic media by the co-polymerization of isocyanate terminated poly(propylene glycol) with hydroxyl-terminated lignin.<sup>124</sup> Compared to kraft lignin and organosolv lignin, lignosulfonate displayed better sensitivity in this application, which can be attributed to the presence of sulfonic acid groups with the lowest  $pK_a$  among these lignins. Nevertheless, one of the major drawbacks of these materials as potential precursors for the fabrication of selective membranes is the poor control and reproducibility over the final material morphology due to the uncontrolled nature of polycondensation reactions, which usually results in partially crosslinked materials that are difficult to recycle.<sup>125</sup> To address this shortcoming, one option could be to use controlled polymerization techniques such as ATRP, but then a careful selection of monomer and reaction parameters (*e.g.* Cu source, solvent and ligand)<sup>126</sup> would be necessary in order not to compromise the production cost, which ultimately can hamper the potential use of lignin in the preparation of these materials.

Chemical modification of lignin has also proved to be an efficient approach to synthesize stimuli-responsive materials for sensing applications. In this sense, Xue *et al.* developed a ratiometric fluorescent pH-sensitive probe by grafting rhodamine B to sodium lignosulfonate.<sup>127</sup> The resulting modified lignin showed a rapid response based on a conformational

change in the Rhodamine moiety to pH variations (from 4.6 to 6.2 with a  $pK_a$  of 5.35) which was then exploited for the detection of acidic organelles. The biological studies showed good biocompatibility of the resulting probe and the ability to differentiate normal cells (HL-7702) from cancer cells (SMMC-7721, HepG2). Although these pH-sensitive probes showed potential in sensor applications, the possibility to target the delivery of drugs to determined sites<sup>128</sup> by chemical modification should be considered for potential nanotheranostic applications as has been previously demonstrated with LCQDs.<sup>87</sup> On the same stream, kraft lignin have also been used as a template to graft porphyrins, and generate lignin–porphyrin polymers (Al-CTPP) with an extension of UV-vis absorbance and photoluminescence regions of lignin together with an enhancement of solvent compatibility of porphyrin in water-dominant environments at different pH.<sup>129</sup> In addition, these lignin–porphyrin polymers showed linear correlations between the absorbance of Al-CTPP and concentration of several heavy metals ions ( $\text{Mn}^{2+}$ ,  $\text{Ni}^{2+}$ ,  $\text{Co}^{2+}$ ,  $\text{Cu}^{2+}$  and  $\text{Zn}^{2+}$ ) suggesting their potential as heavy metal sensor.

**3.1.4 Lignin nanoparticles as platform for sensing applications.** Lignin nanoparticles (LNPs) have been employed for active-substance loading and release applications due to their low cost and functional properties (antioxidant and UV-barrier properties).<sup>130–132</sup> Besides the loading and release of chemical cargo, LNPs are also finding new applications as sensors. In this context, Ma *et al.* recently demonstrated the possibility



to use CEL nanoparticles (CEL-NPs) as sensor for formaldehyde.<sup>133</sup> The basis of the approach relies in the inherent fluorescence emission of CEL-NPs produced by aggregation induced emission effect. Absorption spectra at different concentration of CEL-NPs were used to corroborate the presence of  $\pi$ - $\pi$  aggregates above a concentration of 0.02 mg mL<sup>-1</sup>. In addition, CEL-NPs showed a concentration dependent enhancement of fluorescence after the addition of formaldehyde with a detection limit (LOD) of 8  $\mu$ M, which is comparable to conventional synthetic fluorescent sensors of formaldehyde.<sup>134</sup> Later, Xue *et al.* demonstrated an elegant and easy preparation of alkali lignin-coated Ag-nanoparticles using Ag<sub>2</sub>O as silver precursor, DMSO as solvent and a Lewis acid catalyst,<sup>135</sup> and so avoided the use of harsh reducing agents such as NaBH<sub>4</sub>, thiols or sodium hydroxide.<sup>136,137</sup> The resulting AL@Ag NPs were also applied as calorimetric sensor for Hg<sup>2+</sup> at neutral pH, demonstrating a fast and high specificity towards this analyte in a wide range of concentrations (0.2–20 ppm), similar to classical sensors described for Hg from renewable resources such as chitosan (Fig. 6a–c).<sup>138</sup> In the same domain, Ag NPs have also been synthetized using lignin as a reducing and capping agent for the colorimetric sensing of nickel (Ni<sup>2+</sup>)<sup>139</sup> and mercury (Hg<sup>2+</sup>).<sup>140</sup>

Despite the above examples on the use of LNPs for sensing applications, most of the lignin-based sensor materials presented herein have been designed using crude technical lignins.<sup>43,86,123,124</sup> The main disadvantage of these crude lignins arises from their complex and irregular structure, which often comes in form of a structurally and physicochemical heterogeneous mixture of substances that can jeopardize the final applications. For instance, in the case of LCQDs the structural defects can hamper the fluorescence response<sup>90</sup> and in lignin-based sensors the extent of structural regularity influences the reproducibility and quality of the final materials.<sup>124</sup> Therefore, we urge to exploit the use of LNPs for the development of lignin-based sensors because these colloidal particles

offer the possibility to control the shape, size, and surface topology depending the final application.<sup>132</sup> Moreover, LNPs also hold a great potential to immobilize “target” biomolecules *via* non-covalent interactions and development of new lignin-based biosensor systems in the future.<sup>141</sup>

### 3.2 Biomedical applications

Lignin-based smart materials predesigned for biomedical applications have mainly been based on lignin-based polymers. The grafting polymer is selected to give responsiveness to temperature and pH, the two by far the most well-studied and understood responses in biological systems.<sup>142–144</sup> For instance, thermoresponsive lignin-based materials usually incorporate in their structure polymers with lower critical solution temperature (LCST), which is the lower boundary for demixing *via* coil-globule transition mechanism.<sup>144</sup> Below the LCST, the polymer chains exist as random coils due to mainly hydrogen bond interactions between polymers and water, forming one homogeneous mixed phase. Above the LCST, the phase separation occurs due to a collapse of the polymeric chains to globular structures. This temperature transition has been exploited in loading and delivery of active compounds or to change the morphology of lignin-based hydrogels. In the case of pH as target stimuli, lignin-based polymers either act as sacrificially solubilized polymers or incorporate polymers with pH-responsive compounds that have ionizable functional groups capable of donating or accepting protons upon environmental pH changes.<sup>142</sup> This ionization process promotes an imbalance between the hydrophobic/hydrophilic ratio of the material, which disrupts the stability of the nanoassemblies and enhances the release of active compounds.

#### 3.2.1 Lignin-based nano/microparticles and capsules.

Advanced nanomaterials with the ability to encapsulate and release compounds under the application of specific stimuli have received a tremendous attention recently, particularly in the field of nanomedicine.<sup>145,146</sup> In this context, stimuli-responsive polymers have occupied a prominent place owing to their capability to deliver substances of interest into desired locations in response to various different specific stimuli.<sup>147</sup> Recently, lignin has also emerged as an excellent candidate for loading-release applications due to its relatively low toxicity, biodegradability, high stability, and pH-dependent solubility.<sup>130,132</sup> As has been mentioned, lignin-based smart materials for loading/release applications are obtained by the copolymerization or modification with sensitive monomers such as acrylic acid (sensitive to pH),<sup>142</sup> or *N*-isopropylacrylamide (NIPAM)<sup>143,144</sup> (sensitive to temperature) among others<sup>148–150</sup> (Table 2). However, it is important to mention that lignin can also be considered as a smart material of potential interest by itself. For instance, LNPs which have often been employed as carriers for active substances have showed a pH-dependent stability related to their surface charge (decreasing  $\zeta$ -potential with increasing pH). This trait has been exploited in loading and releasing of different active substances (drugs, agrochemicals, *etc.*) at different pH values.<sup>151,152</sup>

Chemical modification of lignin instead of the polymer grafting strategy has also been demonstrated to be a

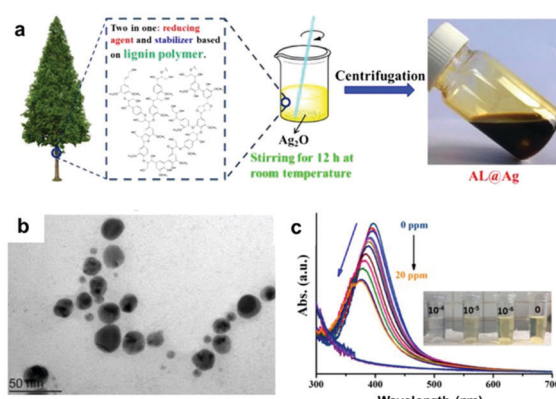


Fig. 6 LNPs as sensor materials: (a) schematic preparation of alkali lignin-coated silver NPs (AL@Ag); (b) a TEM image of AL@Ag particles; (c) UV-vis spectra of AL@Ag particles as sensors for Hg<sup>2+</sup> (from 0 to 20 ppm of Hg<sup>2+</sup>) with a decreasing UV-absorption with increasing Hg<sup>2+</sup> concentrations, and photographs of the color change process demonstrating the detection Hg<sup>2+</sup> at low concentration (10<sup>-4</sup> M). Adapted with permission from ref. 135. Copyright © 2018, American Chemical Society.



**Table 2** Lignin-based smart materials used for the load and release of drugs and other species

Carrier material	Loaded substance	Stimuli-response	EE [%]	Ref.
LNPs	Budesonide	pH	35	151
LNCs	Coumarin-6	pH	84	153
Lignin-g-PEG-PHIS NPs	BZL	pH	50–57	150
lig-His NPs	HCPT	pH	15	154
Succinylated lignin	4-Acetomido-phenol	pH	n.a.	155
Lignin-g-PMMA	IBU	pH	84	156
Lignin-g-PDEAEMA NPs	Decane	CO <sub>2</sub> /N <sub>2</sub> gas	n.a.	149
Lignin-g-PNIPAM NPs	<i>trans</i> -RSV	T	n.a.	144

LNPs-lignin nanoparticles; LNCs-lignin nanocapsules; lig-His-lignin modified with histidine.

useful route towards pH-responsive LNPs for drug delivery applications.<sup>153–155</sup> For instance, Chen *et al.* synthesized pH-responsive lignin-based nanocapsules with the ability to load and release hydrophobic model compounds.<sup>153</sup> In their approach, lignosulfonate was modified with allyl groups in a classical esterification reaction followed by the preparation of the nanocapsules *via* an interfacial miniemulsion reaction, in which the modified lignin reacted with an acid-labile thiol-based crosslinking agent at the interface of miniemulsion droplets to form the nanocapsules through a thiol-ene coupling reaction (Fig. 7a and b). The resulting capsules exhibited a particle size ranging from 100 to 400 nm and their potential application as nanocarriers was evaluated using coumarin-6 as a hydrophobic model compound. The entrapment efficiency (EE) was determined to be 84%, demonstrating a high loading concentration of this system (0.713 mmol g<sup>−1</sup> based on the weight of the modified lignosulfonate). In addition, release

studies from coumarin-6 loaded nanocapsules under neutral (pH = 7.4) and slightly acidic (pH = 4.0) conditions revealed a higher release rate under acidic (60%) compared to neutral (40%) conditions after 48 hours. The difference in the release rates suggests hydrolytic response of the acid-labile  $\beta$ -thiopropionate cross-linkages, which makes these lignin-based nanocapsules promising nanocarriers for drug delivery systems. Later, Zhao *et al.* reported the synthesis of lignin-histidine ( $\text{l-His}$ ) conjugates through the amination reaction between lignin and histidine.<sup>154</sup> After the conjugation,  $\text{l-His}$  showed the ability to self-assemble in water to form homogenous nanoparticles with an average diameter of 30–40 nm, encapsulate hydroxycamptothecin (HCPT) as a drug model with moderate EE values (40%) and triggered release in different media. In addition, carboxylation of lignin has also proved to be an efficient approach for the fabrication of pH-responsive LNPs for controlled release.<sup>155</sup> Figueiredo *et al.* reported the synthesis of complex pH-responsive LNPs for drug delivery and biomedical applications.<sup>150</sup> In a first stage, kraft lignin was carboxylated in order to obtain carboxylated lignin nanoparticles (CLNPs) with an increased amount of carboxyl groups as reactive sites for grafting PEG, polyhistidine (PHIS) and a cell-penetrating peptide *via* EDC/NHS peptide coupling chemistry. The resulting nanoparticles showed an increased circulation in the bloodstream and also pH-responsive behavior. Cytotoxicity studies revealed a high biocompatibility with > 80% of cell viability and the ability to load (with an EE corresponding to 50%) and release benzazulene (BZL) as a model drug compound under physiological (pH = 7.4) and acidic (pH = 5.5) conditions with higher release rates in acidic media. Furthermore, *in vivo* studies also proved the high selectivity of this system through a lower release of BZL in

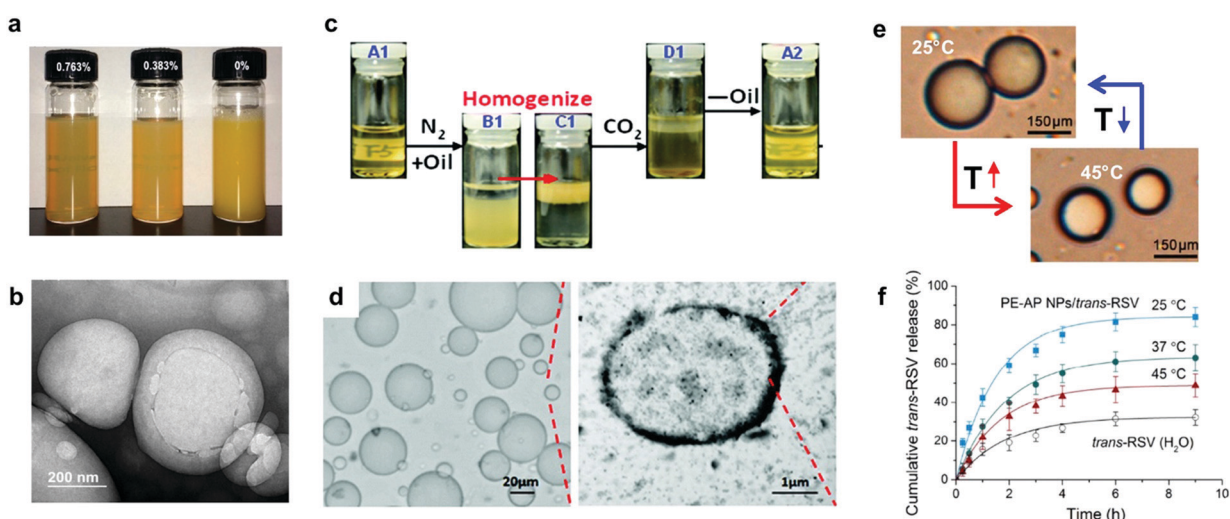


**Fig. 7** Lignin-based smart materials for loading and release applications: (a) appearance of a miniemulsion after 3 min of sonication with 0.76, 0, 0.38, and 0 wt% of sodium dodecyl sulfate (SDS) as surfactant; (b) lignin nanocapsules with broken shells produced during the emulsification process. Adapted with permission from ref. 153. Copyright © 2016, American Chemical Society. (c) Cycle of N<sub>2</sub>/CO<sub>2</sub>-triggered emulsified/demulsified lignin-g-PDEAEMA Pickering emulsion; (d) optical microscope and TEM images of a Pickering emulsion prepared using lignin-g-PDEAEMA with an aqueous/oil volume ratio of 4 : 1. Adapted with permission from ref. 149. Copyright © 2014, Royal Society of Chemistry. (e) Optical micrographs of droplets from lignin-g-PNIPAM NPs stabilized emulsions (0.1 wt%) at 25 °C and 45 °C; (f) cumulative thermal-controlled release of *trans*-RSV. Adapted with permission from ref. 144. Copyright © 2019, American Chemical Society.



physiological environment, causing less toxic effects to the normal cells than to the targeted tumorous cells.

pH-Responsive lignin-based micellar nanoassemblies with the ability to load ibuprofen (IBU) at high EE (84%), have also been recently reported by grafting methacrylic acid (MMA) to lignin through a free radical polymerization process.<sup>156</sup> The resulting lignin-g-PMMA was able to self-assemble into micelles (diameter approximately 100 nm) and control the release of IBU. *In vitro* release experiments showed only 16% release of IBU in a simulated gastric fluid (pH 1.5), while in a neutral simulated intestinal fluid (pH 7.4) an accumulated release of 81% was determined. This tunable release of IBU can be rationalized by the ionization of acidic groups at low pH, which protects the corona of the micellar nanoassemblies and avoids the release of the active compound at low range of pH values. *In vivo* studies furthermore demonstrated a certain inhibitory effect towards proliferation of colon cancer cells (NIH-3T3), while presenting low cytotoxicity to normal cells. Similar pH-responsive release processes have been observed in alkali lignins by the ionization of carboxylic groups.<sup>151,155</sup> However, it is important to mention that this release behavior also depends on the solubility properties of the loaded compounds as in the case of coumarin-6 that was released more efficiently under mildly acidic conditions compared to neutral pH.<sup>153</sup>

Qian *et al.* also developed another type of smart LNPs by grafting dimethylaminoethyl acrylate (DEAEMA) monomer into a kraft lignin core by ATRP.<sup>149</sup> The resulting lignin-g-PDEAEMA copolymer could be easily dispersed in water to form LNPs upon CO<sub>2</sub> gas bubbling, and to initiate aggregation and eventual precipitation by N<sub>2</sub> gas bubbling. This CO<sub>2</sub>/N<sub>2</sub> switching ability is conferred by the presence of DEAEMA based on a reversible protonation of amine groups catalyzed by the acidic CO<sub>2</sub>, and is tailored by the graft density and chain length of the DEAEMA units. These modified LNPs showed a promising potential as surfactants for Pickering emulsions. Stable Pickering emulsion were prepared using decane as an oil phase with only 1 wt% of LNPs; the emulsions remained stable for more than one month without any phase separation and exhibited a gas triggered de-emulsification/re-emulsification behavior. CO<sub>2</sub>/N<sub>2</sub> bubbling cycles demonstrated that bubbling with CO<sub>2</sub> allowed a complete emulsion breaking with the consequent phase separation, while N<sub>2</sub> bubbling resulted in re-emulsification of the mixture (Fig. 7c and d). The authors claimed that such smart lignin surfactants could be of great potential as drug delivery systems, but no drug release and cytotoxicity studies were demonstrated. More recently, Dai *et al.* reported the synthesis of thermoresponsive lignin nanoparticles by grafting NIPAM into lignin *via* ATRP and self-assembly in water, successively.<sup>144</sup> These copolymer nanoparticles were used as smart surfactants to stabilize *trans*-resveratrol (*trans*-RSV)-containing palm oil in water Pickering emulsion droplets. Combining the thermoresponsive and UV resistance properties in lignin-g-PNIPAM NPs, this stimuli-responsive Pickering emulsion system showed an improved performance on the controlled release and light stability of *trans*-RSV in comparison to other systems based on polymeric nanoparticles<sup>157,158</sup> (Fig. 7e and f).

Additionally, these Pickering emulsions showed remarkably good biocompatibility (around 100% cell viability of A549 cells at a wide range of concentrations), improved solubility and antiradical efficiency as compared to free *trans*-RSV in water. The inherent combination of lignin properties (UV-protection) together with the thermoresponsive behavior of NIPAM could be of renewed interest for drug delivery systems for the storage of light-sensitive and poorly water-soluble drugs. In the same vein, Peng *et al.* also harnessed the UV-shielding properties of lignin to fabricate avermectin-containing emulsions using microspheres with tunable surface charge and composed of sodium lignosulfonate and cetyltrimethylammonium bromide (CTAB).<sup>159</sup> The resulting emulsions showed sustained release behavior (ranging from 56–80% in 60 h), and an improved light-storage stability of 2.18–2.96 times higher in comparison to commercial avermectin emulsifiers.

As has been discussed above, lignin-based smart material for drug loading and release applications have mainly been based on the development of lignin-based polymers with the ability to form pH-responsive LNPs.<sup>150,153–155</sup> Indeed, pH is without any doubt one of the most attractive stimuli since different parts of the body and cellular compartments present some variations in pH values which could be exploited to trigger selective release of drugs.<sup>160</sup> However, there are also many other stimuli in biological systems which can be exploited as is the case of redox potential,<sup>161</sup> endogenous gases<sup>162</sup> or certain enzymes,<sup>163</sup> which have been already integrated and employed in classical stimuli-responsive polymers,<sup>147</sup> while literature is lacking such reports on lignin-based smart materials. Therefore, we urge to expand the development lignin-based polymeric materials integrating other attractive stimuli or even the combination of them in order to generate materials with synergistic simultaneous action as in the case of their predecessor polymeric materials.<sup>164–166</sup> Another relevant issue is that the systems described above are based on covalent functionalization of lignin with the final aim to introduce stimuli-responsive behavior and control over the release properties. However, non-covalent functionalization is also an appealing approach in terms of synthetic preparation and potential reversibility of functionalization, and therefore should also be considered as an efficient alternative for the design of stimuli-responsive materials. For instance, LNPs with negative surface charge have been used to adsorb cationic polymers such as poly(diallyldimethylammonium chloride) (PDADMAC),<sup>167,168</sup> chitosan<sup>169</sup> and water-soluble cationized lignin.<sup>170</sup> The resulting LNPs with a cationic surface charge have been demonstrated as efficient supports for enzyme immobilization and biocatalysis,<sup>168,171,172</sup> but could be also considered as a promising platform for the future development of smart confined biocapsules not only for drug release applications but also for the design or more complex materials such as bio-inspired nanomotors, already developed with conventional polymeric materials.<sup>173,174</sup>

**3.2.2 Lignin-based smart hydrogels.** Another important class of stimuli-responsive lignin materials with potential for drug delivery applications and tissue engineering is lignin-based



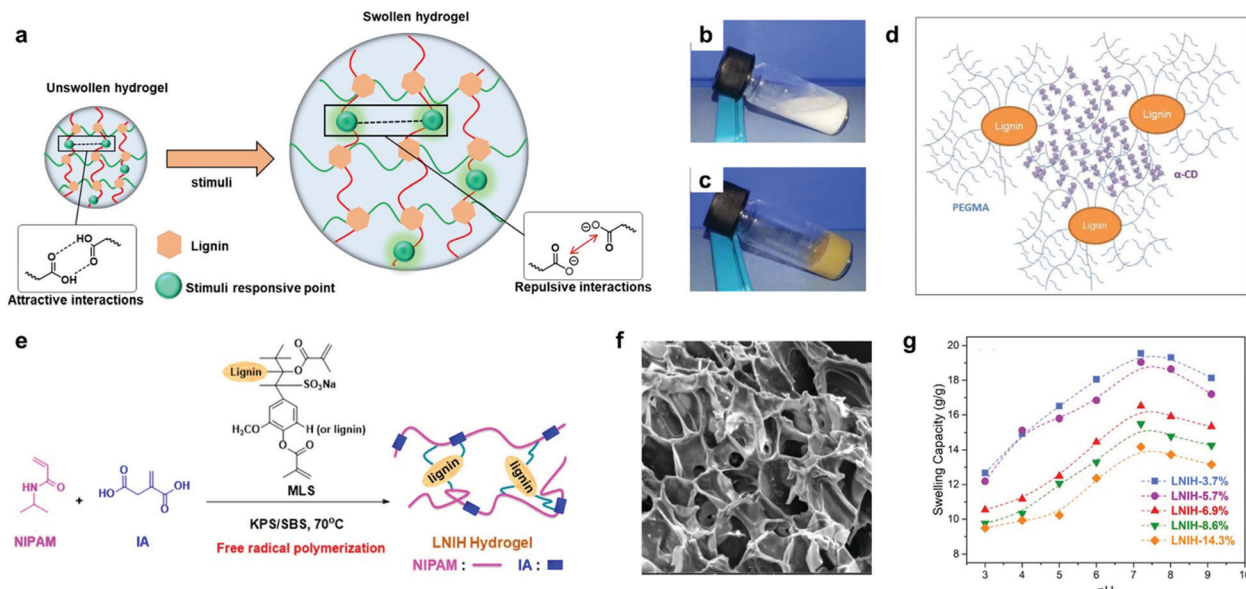


**Fig. 8** Lignin-based smart hydrogels: (a) depiction of swelling behavior of lignin-based smart hydrogels upon the application of a specific stimuli (pH-dependent lignin-based hydrogels is shown as example, where the stimuli applied corresponds to pH variation). (b) photographs of the inclusion complex suspension of PEG 10/10 (10% PEGMA + 10%  $\alpha$ -cyclodextrin); (c) digital images of lignin-based hydrogel (2% lignin-g-PEGMA + 10%  $\alpha$ -CD); (d) schematic representation for the proposed structure of a lignin-based supramolecular hydrogel by inclusion complexation between lignin-g-PEGMA and  $\alpha$ -CD. Adapted with permission from ref. 176. Copyright © 2015, American Chemical Society. (e) Synthetic approach for the lignin-based hydrogels via free radical polymerization. Note that the lignin structural model MLS should be considered only as an illustration. (f) SEM image of lignin-g-PNIPAM hydrogel containing lignin in a 14.3% wt; (g) swelling capacities of lignin-g-PNIPAM with increasing content of lignin (from 3.7 wt% to 14.3 wt%) at different pH values at 25 °C. Adapted with permission from ref. 142. Copyright © 2018, American Chemical Society.

hydrogels. Their porous structure shares similarities with the biological extracellular matrix, and the stimuli-dependent swellability in water plays an important role for drug delivery applications (Fig. 8a).<sup>142,143,148</sup> As smart biomaterial, lignin-based hydrogels have been programmed to be sensitive to pH and temperature, the two most common stimuli employed in biomaterial and biomedical applications. By grafting temperature-sensitive monomers into a lignin core, thermo-responsive lignin-based hydrogels have been synthetized for phase transitions at close to body temperatures. Diao *et al.* reported the synthesis of termogelling copolymers by the copolymerization of NIPAM, PEG and poly(propylene glycol) (PPG) using ATRP as the polymerization methodology.<sup>148</sup> The resulting copolymers exhibited a thermogelling behavior at 32–34 °C with the consequent formation of the corresponding hydrogels. The lignin-based hydrogels showed a low gelation concentration in the range of 1.3 to 2.5 wt% and highly tunable mechanical and rheological properties by simple modification of the weight ratio of lignin (from 5% to 40%) in the system. Feng *et al.* also reported the synthesis of thermo-responsive lignin-based hydrogels by grafting carboxylated lignin with NIPAM using *N,N'*-methylenebisacrylamide as a crosslinker and hydrogen peroxide as an initiator.<sup>175</sup> The resulting lignin-based hydrogels showed a low critical solution temperature (LCST) of 32 °C that dramatically decreased the swelling ratio (from >1000% to 200%), indicating potential use as smart materials for biomedical applications. In another work, Kai *et al.* also introduced lignin-based hydrogels with thermo- and

mechanical responsiveness by the preparation of lignin grafted copolymers with PEGMA.<sup>176</sup> The resulting lignin copolymer could self-assemble into supramolecular hydrogels when mixed with  $\alpha$ -cyclodextrin ( $\alpha$ -CD) via reversible host-guest inclusion complexation. The authors described that as low as 1 wt% of lignin-based copolymers were able to form stable hydrogels at body temperature and the lignin core was important in the gelation process, since it provided control over the oscillation strain, which ultimately defines the transition from a solid-like hydrogel into a liquid-like state (form/state-response) (Fig. 8b–d). Additionally, these hydrogels showed a good biocompatibility and potential for tissue engineering materials.

More recently, temperature- and pH-responsive lignin-based hydrogels have also been synthetized via free radical polymerization.<sup>142,143</sup> Jin *et al.* reported the preparation of a lignin-based hydrogel by the copolymerization of NIPAM, itaconic acid and methacrylate functionalized sodium lignosulfonate.<sup>142</sup> The prepared hydrogels showed a reduction in the swelling capacity (from 31.6 to 19.1 g g<sup>-1</sup>) with the increase of lignin content (from 3.7% to 14.3%), revealing a lignin-dependent water absorption. In addition, phase transition temperature values around the body temperature together with a broad pH responsive range (from pH 3 to 9) make them interesting candidates for drug release applications (Fig. 8e–g). However, the poor control over the material structure generally resulting from free radical polymerization methodologies and the difficult reproducibility in the synthesis could be critical barriers to overcome when scaling up the production.

**3.2.3 Technical challenges in lignin-based smart materials for biomedical applications.** Although the above studies demonstrated the potential of using lignin in the fabrication of biomedical materials, there are also some concerns that need to be addressed. For instance, the selection of a lignin source is a critical question since many technical lignins contain impurities such as ions coming from the extraction process which could be toxic.<sup>36</sup> The use of alternative lignins as is the case of CEL will reduce the problem but not fully resolve it. Therefore, it is mandatory to increase the purity of the starting materials and understand their reactivity in order to control the cytotoxicity of these lignin-based materials.<sup>177,178</sup> Other consideration is related to improving the methodology to synthetize LNPs. These nanostructures are usually synthetized by solvent-exchange methodology which involves the use of harmful organic solvents such as THF<sup>167,179</sup> and acetone,<sup>180</sup> which could jeopardize the final application. Recently, first steps to address this issue have been reported with the use of ethanol as an alternative solvent. However, the concentration of LNPs that can be prepared is only about one fifth from that achieved with THF or acetone.<sup>151,181</sup> In this context, expanding the limited palette of solvents suitable for the preparation of LNPs and including new non-toxic solvents is important.<sup>182</sup> Especially biomass-derived solvents such as ethyl lactate already used in the production of polymeric materials could be assessed in the future.<sup>183</sup>

Although frequently neglected, another important consideration about these lignin nanomaterials is their biodegradability. While many of the reports focus strictly their attention on the cytotoxicity and biocompatibility studies, the biodegradability of these materials remains largely unexplored. It is well known that lignin can be partially decomposed by enzymes,<sup>16,184</sup> but most of these smart materials described above are based on chemical modification of lignin, which probably disrupts the degradability process. For instance, cross-linked lignin materials are likely drastically less biodegradable and the absence of phenolic hydroxyl groups hinders accessibility of these primary sites in enzymatic degradation processes. Therefore, more data should be collected regarding the biodegradability of lignin-based smart materials and the nature of the degradation products.

### 3.3 Shape-programmable materials

Shape memory materials are capable of fixing temporally “programmed” shapes and returning to the original shape by the application of external stimuli such as temperature,<sup>185</sup> light,<sup>186</sup> electricity,<sup>187</sup> moisture<sup>188</sup> or magnetism.<sup>189</sup> These materials are widespread in the field of polymer science due to their attractive properties for biomedical applications,<sup>85</sup> such as polymeric-based actuators which have been used as artificial muscles for the fabrication of blood vessel connections or microvalves to regulate the urinary incontinence, among others.<sup>190–192</sup> Lignin by itself displays a high glass transition temperature ( $T_g$ ) (from 90 °C to 145 °C, depending on the source and type of isolation process), owing to its rigid aromatic backbone and strong intra and intermolecular interactions (mainly hydrogen bonding and  $\pi$ - $\pi$  stacking interactions). When lignin is modified for use as a

macromonomer, this inherent nature usually leads to materials with thermosetting characteristics, which could be further designed to act as shape memory materials for smart applications. In this context, Xu *et al.* reported the synthesis of lignin-based thermosets exhibiting tunable mechanical properties and shape memory behaviour.<sup>193</sup> These thermosets were synthetized in a simple approach using crude kraft lignin without any chemical modification, citric acid as a cross-linking agent and PEG as a reactive diluent and soft segment. PEG facilitated the cross-linking reaction and balanced the final mechanical properties by increasing the dispersion of all the components, but also provided materials with excellent shape memory characteristics such as 99% recovery rate and 95% fixity ratio, which indicate how well the shape is recovered and the ability to fix the mechanical deformation, respectively. These values are comparable to those reported for other thermoset composites based on epoxy resins or polybenzoxazines.<sup>194</sup> Although this approach is attractive in terms of synthetic preparation and low cost-production, there still remains a major concern related to the difficult recyclability of thermosetting materials, since most of them are disposed of *via* incineration or landfilling.

To overcome the rigidity issue of lignin, the incorporation of vitrimer chemistry into the preparation of thermosets has gained attention.<sup>195,196</sup> Incorporation of dynamic covalent linkages that can be stimulated by heat or UV light into cross-linked structures results in rearrangements in the material topology, imparting improved malleability and recyclability (Fig. 9a).<sup>197,198</sup> In this stream, Zhang *et al.* reported the first example of lignin-based vitrimer material with shape memory behavior by the reaction of ozonated lignin with sebacic acid derived epoxy in the presence of a zinc catalyst (Fig. 9b).<sup>199</sup>  $Zn^{2+}$  ions catalyzed transesterification reactions in the cross-linked network *via* associative exchange pathway (Fig. 9a), which resulted in a thermoset material with shape-memory, self-healing and malleability properties (Fig. 9c). Moreover, these lignin-based vitrimers revealed interesting features as adhesives when adhered to aluminum sheets, with a lap-shear strength value of 6.3 MPa comparable to epoxy-based adhesives such as the commercial epoxy glue with a lap-shear strength of 8 MPa,<sup>200</sup> or bisphenol A-based epoxy adhesives with a lap-shear strength values of 4–6 MPa<sup>201</sup> (Fig. 9d).

However, perhaps one of the main disadvantages of this approach relies in the narrow scope of functional groups presents in lignin, mainly limited to hydroxyl and phenolic groups. This fact could restrict the introduction of a wide palette of interesting dynamic covalent linkages based for instance on amino functional groups and urethane chemistry.<sup>198,202</sup> Chemical modification of lignin (Fig. 3a) could of course be a possibility to increase the scope of dynamic covalent linkages, albeit at a cost of an additional synthetic step.

**3.3.1 Lignin-based elastomeric and thermoplastic elastomer materials with shape-memory behaviour.** Lignin-based elastomeric and thermoplastic elastomeric materials with tunable shape memory properties have emerged in the last few years.<sup>203–208</sup> These materials are based on the use of lignin as a hard segment “plastic phase” and the grafting of polymers with



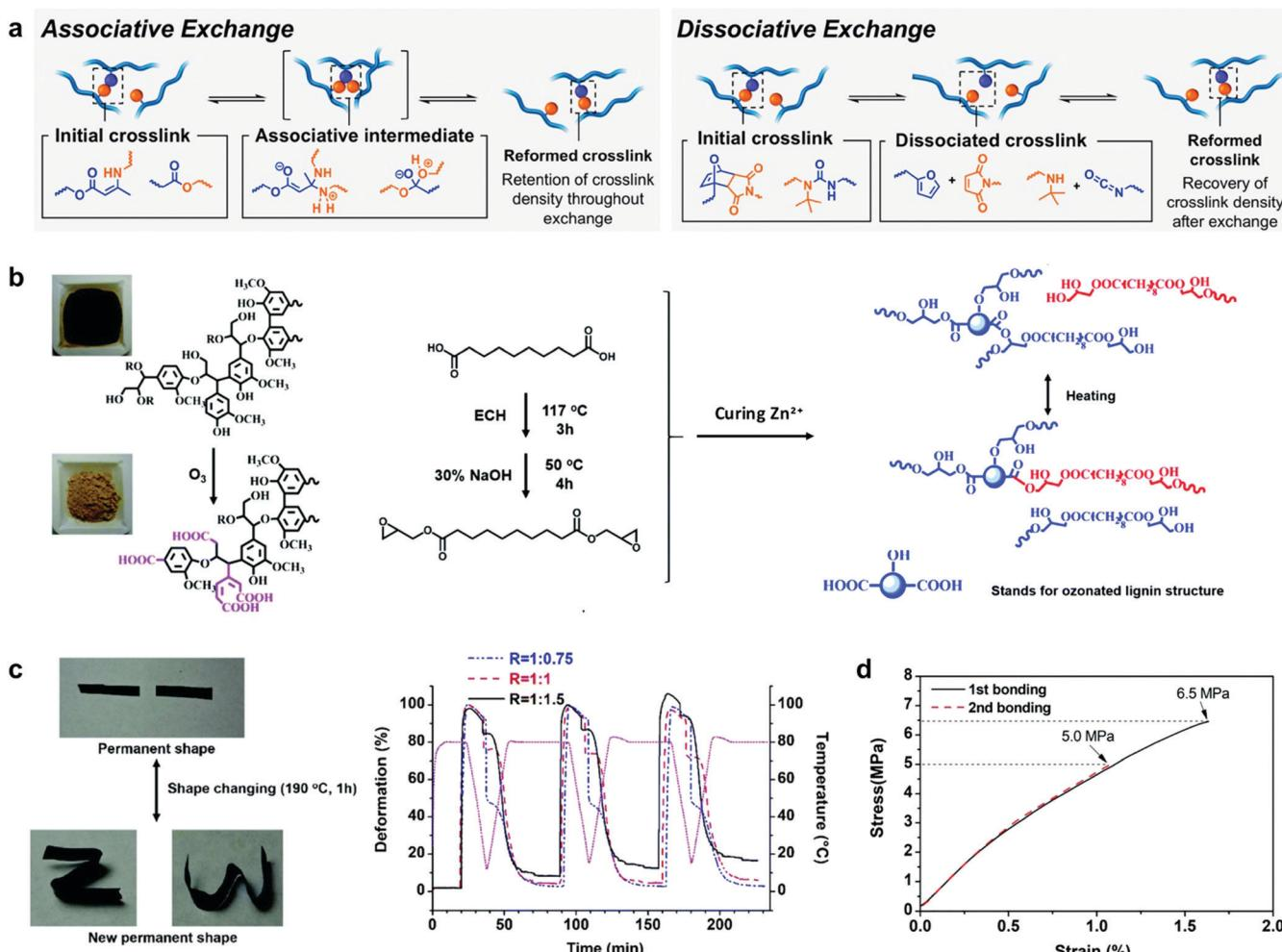


**Fig. 9** Lignin-based shape-programmable materials: (a) depiction of associative and dissociative bond exchange pathways for covalent adaptable networks by vitrimer chemistry. Adapted with permission from ref. 195. Copyright © 2019, American Chemical Society. Lignin-based vitrimer material with shape-memory behavior: (b) schematic diagram of the preparation of lignin-based vitrimer and its reconstruction *via* transesterification reactions; (c) shape changing and consecutive shape memory cycles for different compositions of the lignin-based vitrimer material; (d) the lap shear test of lignin-based vitrimer as an adhesive on coarsened aluminum sheets with different bonding times. Adapted with permission from ref. 199. Copyright © 2018, Royal Society of Chemistry.

low  $T_g$  as a “soft phase” in cross-linked-like structures. One of the two phases act as a “switch” capable of undergoing a phase transition or change in conformation, while the other remains immobile and allows the material to “remember” its original shape. Most of these lignin-based materials have been programmed to be sensitive to temperature, based on the combination of the glass transition of grafted polymers with lignin, together with the reversible dissociation of self-complementary non-covalent bonding (e.g. hydrogen bonding) and by controlling the cross-linking density.<sup>203,204,208</sup>

Pioneering works in the development of these lignin-based materials were reported by McDonald’s group, who synthesized thermally-stimulable shape memory elastomers from lignin and glycerol-adipic acid based hyperbranched prepolymers.<sup>203</sup> In the first step, hyperbranched prepolymers were synthesized by melt polycondensation reaction of glycerol, adipic acid and the addition of di- and tri-functional amines as cross-linking points.

After that, the prepolymers were reacted with soda lignin *via* bulk polycondensation reaction to afford the corresponding shape memory elastomers. The obtained elastomers presented tunable  $T_g$  as well as shape transition temperature values ranging from  $-10\text{ }^\circ\text{C}$  to  $40\text{ }^\circ\text{C}$  by varying the amount of the amine additives. Dynamic mechanical analysis (DMA) *via* a stress controlled cyclic thermomechanical test revealed that the materials exhibited a dual shape memory behavior with 94% recovery rate and 99% fixity rate. Later, the same group reported the preparation of lignin-based elastomeric materials with triple shape memory by the polymerization of soda lignin with a new hyperbranched poly(ester-amine-amide) containing amine cores and amide linkages.<sup>204</sup> The presence of a broadened  $T_g$  in these materials revealed a mixed phase by the coexistence of two networks within lignin (polyester-amine and polyester-amine-amide) comprising covalent and physical cross-linked points, which were responsible for the triple shape memory

behavior. As in the previous case, the shape memory behavior of these materials was evaluated by a stress-controlled cyclic thermomechanical test, which confirmed a reasonable triple shape memory behavior (fixity rate reached 41% and 92%, while recovery rates reached 40% and 86%, respectively for the 1st and 2nd shape recovery stage). These results were explained on the ground of the combined effect of increased covalent cross-linking and dissociation of self-complementary physical hydrogen bonding present in the network. Interestingly, it was also found that the first recovery stage was associated to the lignin-poly(ester-amine) network and the second one to the lignin(ester-amide) segments, which indicates the important role of physical cross-linking to obtain these types of materials. Although these were the first examples of lignin-based elastomeric shape memory materials with multiple shape memory behavior, the properties are far behind those of conventional polymeric materials (fixing and recovery rate up to 95%).<sup>209,210</sup> In this sense, increasing the polymer compatibility and dispersibility of lignin seems to be crucial aspects, in addition to the use of sacrificial bonds capable to dissipate energy, eliminate stress, and promote the orientation of chain segments, which are all appealing strategies towards the development of future materials.<sup>208,211</sup>

More recently, Liu *et al.* reported the synthesis of lignin-cross-linked polycaprolactone (PCL) copolymers as elastomeric materials with shape memory behavior using lignin as a core segment for the cross-linking.<sup>205</sup> This approach was based on a

thiol-ene coupling reaction between a thiol terminated four-arm PCL with an alkene-modified kraft lignin. The prepared lignin-copolymers revealed tunable melting temperatures ( $T_m$ ) by the variation of lignin content (from 10 to 40 wt%). Moreover, the authors claimed that the shape memory process is efficient and the recovery is immediate which could make these materials interesting candidates for biomedical applications, in which self-expansion times of less than 60 seconds are required.<sup>212</sup> However, the reported phase transition temperature was found to be 80 °C, which is unfit for biomedical applications, in which activating temperatures are instead governed by the thermoregulations of the human body.<sup>213</sup>

Lignin-based thermoplastic elastomers (Lig-TPEs) with shape memory behavior combine both thermoplastic and elastomeric properties, together with a stimuli responsive behavior.<sup>25,41</sup> In this context, Nguyen *et al.* recently reported the preparation of Lig-TPEs based on acrylonitrile–butadiene–lignin composites (ABL) with a high lignin content (40–60 wt %), *via* cross-linking of lignin with an acrylonitrile–butadiene rubber (NBR) by a thermal compounding process.<sup>206</sup> The resulting ABL materials showed excellent shape memory behavior as a consequence of chemical cross-links in the inherent structure of NBR and the intrinsic networked structures of lignin, which complemented physical cross-links formed by hydrogen bonds within lignin and nitrile rubber molecules (Fig. 10a and b). In addition, the authors also reported the preparation of a programmable and

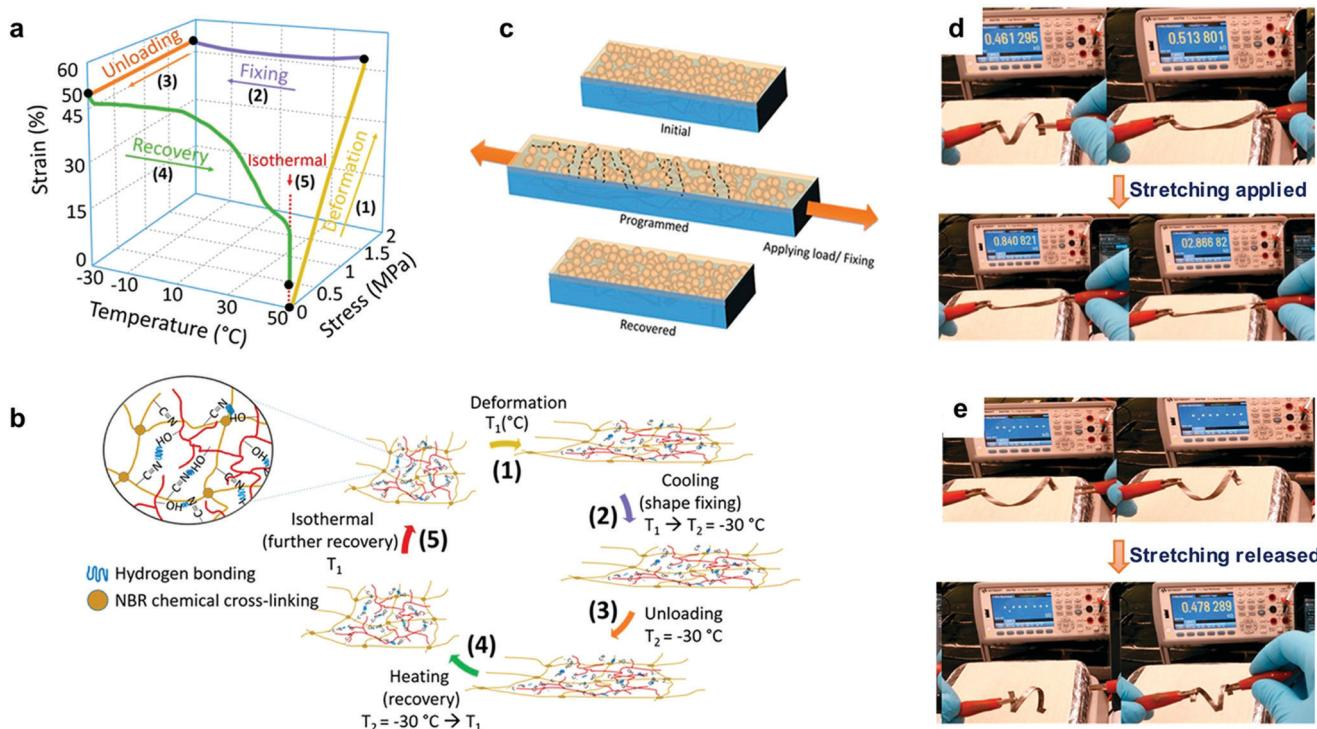


Fig. 10 Lig-TPEs as shape programmable material: (a) three-dimensional graph of one cycle of deformation, fixing and recovery in ABL material; (b) the corresponding programmed shape recovery of ABL networks with a magnified view showing a network structure of a nitrile–butadiene elastomer (NBR) and lignin in the presence of hydrogen bonds formed by  $-\text{OH}$  and  $-\text{C}\equiv\text{N}$  groups; (c) principle of switchable and programmable electrical conductivity of a silver nanoparticle layer assembled on a shape-memory substrate; (d and e) initial, after fixing/shape programming, and after restoring shape and resistance of the shape-programmed electrically conducting material. Adapted with permission from ref. 206. Copyright © 2018, American Chemical Society.



switchable conducting material by depositing silver (Ag) nanoparticles on the surface of an ABL specimen. After the coating process, this new material could be shape-programmed to respond to an external stress at ambient temperature for multiple times, revealing an increase in the resistance from 0.46 k $\Omega$  to 2.86 k $\Omega$  during the process (Fig. 10d). Moreover, after the applied external force was switched off, the shape-programmed sample recovered its original shape and resistance (0.47 k $\Omega$ ) which was associated to a reversible breaking of particle percolation (Fig. 10c and e). These new shape-programmable conductive materials with the ability to sense changes in the resistance induced by changes in applied stress could be of potential interest for the development of new motion sensors such as human motion tracking sensors.<sup>214</sup> However, further work is required to engineer the  $T_g$  values for these materials (ranging from  $-2.5$  to  $11$  °C) closer to ambient temperatures to broaden their stress-strain sensing window for potential applications. In this context, improvement of thermomechanical properties of these ABL materials (increasing of  $18$  °C in  $T_g$  values and more than  $230\%$  increasing in the storage modulus ( $E'$ )) were later reported by the same group, applying a thermal annealing process, which enhanced the crosslink density by the generation of radicals from lignin.<sup>207</sup> It is important to mention that the obtained materials still maintained good shape memory behavior and therefore this approach could be considered of interest to tune the thermomechanical properties of these Lig-TPEs and make them more attractive for a wide range of applications where high  $T_g$  values are required.

Another approach to improve the mechanical properties and shape memory behavior of Lig-TPEs was reported by Huang *et al.* who used sacrificial bonds based on the presence of Zn-mediated coordination bonds in the interface of lignin and a non-polar elastomeric polyolefin (Fig. 11a and b).<sup>208</sup> The presence of these sacrificial bonds was found to promote the dispersion of lignin with a particle size around 200 nm, but also to improve the interfacial interaction of lignin and polyolefin elastomeric matrix, which results in a more accessible orientation of the chain segments during the stretching with the consequent improvement on shape-memory characteristics of the material (fixing rate and recovery rate values up to 87%). Indeed, the synergistic coordination effect of lignin promoted a

higher energy dissipation together with an improvement of toughness and strength of these Lig-TPEs, rendering them comparable to commercial TPEs such as polyolefin blends-based materials in which the plastic phase comes from petroleum-derived sources.<sup>215,216</sup> Overall, harnessing intrinsic material properties of lignin holds many opportunities for future development of high-performance and cost-effective TPEs.

The development of lignin-based materials with “programmable” shape memory behavior is a fascinating field with multiple potential applications as has been described above. However, it is also important to note that all of the materials presented above are capable of responding to temperature as the only stimulus. In that context, light-driven lignin-based shape memory materials appear as an appealing option in the horizon because light stimuli offer flexibility in terms of spatiotemporal control. One could envision that the development of these materials will logically require the use of light-responsive monomers (*e.g.* azobenzenes) able to produce changes in response to light *via* isomerization processes among others.<sup>217,218</sup> However, it must be noted that some properties that make lignin attractive for other applications such as a high UV-absorbance,<sup>144,156</sup> can play a negative role by the partial or total inhibition of these light-induced processes and affect the final performance of the lignin-based actuator. Therefore, the design of lignin-based smart materials with programmable shape memory behavior need not only focus on the “conception” of the stimuli integration, but also consider the potential interaction of lignin with the applied stimuli and the expected response of the material.

Last but not least, the development of materials with the ability to respond to multiple stimuli, and mimic artificial muscles capable of converting energy from external stimuli to mechanical forces are intriguing challenges that could be addressed with lignin-based shape-programmable materials in the near future. First steps to address these issues have already been taken, with the rational design of lignin-based hydrogel actuators sensitive to pH. The performance of these materials is based on macroscopic changes such as swelling and shrinking upon pH changes. Recently, Dai *et al.* reported a simple approach consisting of a one-step crosslinking reaction of industrial kraft lignin with poly(ethylene glycol)diglycidyl

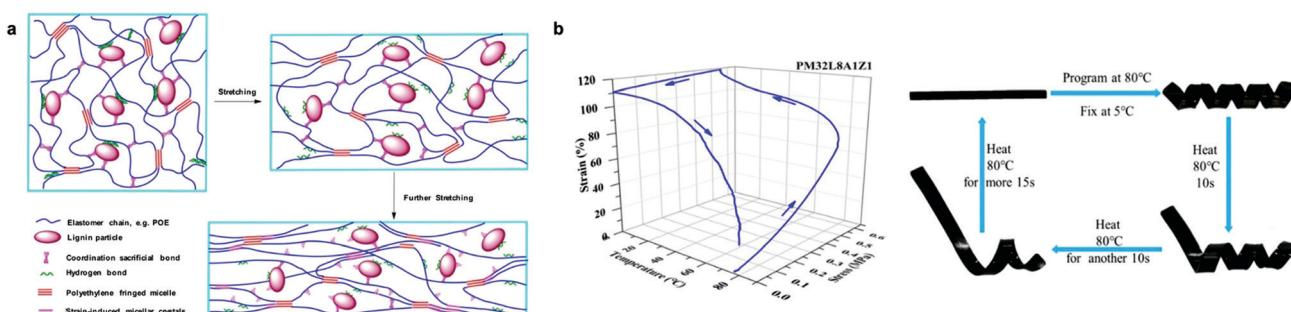


Fig. 11 Lig-TPEs as shape programmable material incorporating sacrificial bonds: (a) schematic representation of deformation mechanism of Lig-TPEs; (b) stress-controlled program and photographs of the shape memory performance of Lig-TPEs. Adapted with permission from ref. 208. Copyright © 2019, American Chemical Society.



ether acting as a crosslinker under basic conditions.<sup>219</sup> The resulting lignin-based hydrogel showed relatively fast (1 min) mechanical actuation by transition between softening/enhancement and straight/bending shapes by alternately immersing the hydrogel in 0.1 M HCl and 0.1 M KOH. Additionally, an intelligent hook and flow control valve based on this system was developed to control the filtration of solutions demonstrating a broader potential of this material. This approach illustrates that a good rational design of low cost lignin-based smart material can also open new avenues for the development of lignin-based actuators.

## 4. Perspective for future development

Lignin-based smart materials have emerged as worthy options for advanced biomaterials because of their intrinsic functional properties and green carbon footprint. Many of the examples discussed in this review demonstrate that lignin-based smart materials stand comparison to conventional stimuli-responsive polymers in sensors, biomedical applications, and shape memory materials. It is thus well rationalized to foresee that lignin-based smart materials will continue to see a rapid expansion towards new materials and applications. It is also important to note that in many of the examples described in this review the stimuli-responsive capabilities are not provided directly by the nature of lignin (*e.g.* lignin-based polymers). This fact can induce a thinking that in some cases the role of lignin is merely secondary and could be eventually easily replaced. However, it is unfair to judge the contribution of lignin in these materials based only on this angle. In most of the cases, a global vision of these systems demonstrated that a rational combination of lignin properties with stimuli-responsive materials can offer the possibility to fabricate systems for a more advanced performance, as is the case of lignin-based smart polymeric materials for drug delivery and light stabilization. We also envision that in a near future the development of all-lignin-based smart materials will be a reality by exploiting the inherent properties of lignin in their different shapes and sizes. For instance, LNPs hold the potential to enable reversible aggregation processes in different solution media which could be used to design new sensors based on aggregation induced emission (AIE) effect.

In fact, there are many prospective materials that can be prepared from lignin precursors such as (nano)materials programmed for degradation, bio-mimicking materials, multi-stimuli responsive systems, and other engineered stimuli-responsive materials (Fig. 12). Future challenges for lignin-based smart materials include gaining a better understanding of structure, isolation, and predictable batch to batch properties of lignin, transformation to “standardized” molecular and nano/micro building blocks, and structure–function relationship in applications. It will also be important to demonstrate scale-up and proof of concept of lignin-based materials to attract industrial activity in this new material domain.

Many prospective applications are linked to the development of lignin-based materials with the ability to interact or mimic biological systems such as selective membranes. These materials are typically composed of biomolecules such as proteins linked to other components that lead to changes in the macroscopic conformation. Many bio-mimicking systems developed so far involve the use of synthetic polymeric nanoparticles,<sup>220</sup> which could instead be formed from lignin.<sup>221</sup> For drug delivery systems it will be important to synthesize materials carrying more than one active substance with potential for site-specific and controlled sequential or simultaneous release. This also includes the possibility to fabricate LNPs with programmable shape memory behavior, which could lead to the preparation of multicompartment capsules (MCCs) mimicking biological cells,<sup>222,223</sup> for instance through phase-separation processes with the inherent possibility to encapsulate several active compounds in the different compartments. Last but not least, as has been discussed in this review, there is potential for future work to address the introduction of multiple and external stimuli in an “intelligent” and predictable manner to generate a new generation of advanced materials. These materials will consist of engineered signaling chains that allow for switching “on” or “off” the corresponding lignin-based device, after the application of a programmable series of stimuli, including potential cascade processes already presented in polymeric systems.<sup>224–226</sup> In summary, the combination of the lucrative properties of lignin nano- and hybrid materials together with the increasing diversity of responsive materials foretell that lignin-based smart materials will be a vibrant area to explore in the future.

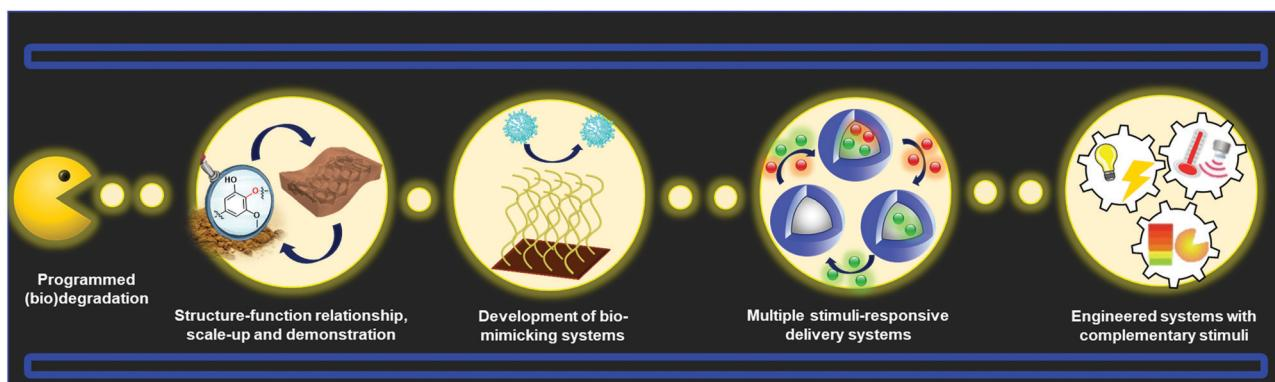


Fig. 12 Future challenges and prospective new frontiers for lignin-based materials.



## Conflicts of interest

There are no conflicts to declare.

## Acknowledgements

The authors acknowledge the Department of Materials and Environmental Chemistry (MMK) for financing this work through the start-up grant awarded to MHS.

## Notes and references

- Declaration of the United Nations Conference on Environment and Development, Rio de Janeiro, Brazil, June 3-14, 1992. [http://www.unesco.org/education/pdf/RIO\\_E.PDF](http://www.unesco.org/education/pdf/RIO_E.PDF), accessed, January, 10, 2020.
- J. K. Hammitt, R. J. Lempert and M. E. Schlesinger, *Nature*, 1992, **357**, 315–318.
- S. A. Miller, *ACS Macro Lett.*, 2013, **2**, 550–554.
- Y. Zhu, C. Romain and C. K. Williams, *Nature*, 2016, **540**, 354–362.
- D. K. Schneiderman and M. A. Hillmyer, *Macromolecules*, 2017, **50**, 3733–3749.
- D. Ghosh, D. Dasgupta, D. Agrawal, S. Kaul, D. K. Adhikari, A. K. Kurmi, P. K. Arya, D. Bangwal and M. S. Negi, *Energy Fuels*, 2015, **29**, 3149–3157.
- C. O. Tuck, E. Perez, I. T. Horvath, R. A. Sheldon and M. Poliakoff, *Science*, 2012, **337**, 695–699.
- Y. Habibi, L. A. Lucia and O. J. Rojas, *Chem. Rev.*, 2010, **110**, 3479–3500.
- N. Lavoine, I. Desloges, A. Dufresne and J. Bras, *Carbohydr. Polym.*, 2012, **90**, 735–764.
- N. M. L. Hansen and D. Plackett, *Biomacromolecules*, 2008, **9**, 1493–1505.
- W. Boerjan, J. Ralph and M. Baucher, *Annu. Rev. Plant Biol.*, 2003, **54**, 519–546.
- K. V. Sarkany and C. H. Ludwig, *Lignins: Occurrence, Formation, Structure and Reactions*, Wiley-Interscience, New York, 1971, pp. 19–38.
- D. M. O’Malley, R. Whetten, W. Bao, C.-L. Chen and R. R. Sederoff, *Plant J.*, 1993, **4**, 751–757.
- Y. Wang, M. Chantreau, R. Sibout and S. Hawkins, *Front. Plant Sci.*, 2013, **4**, 220.
- A. J. Ragauskas, G. T. Beckham, M. J. Biddy, R. Chandra, F. Chen, M. F. Davis, B. H. Davison, R. A. Dixon, P. Gilna, M. Keller, P. Langan, A. K. Naskar, J. N. Saddler, T. J. Tschaplinski, G. A. Tuskan and C. E. Wyman, *Science*, 2014, **344**, 1246843.
- D. Yiamsawas, G. Baier, E. Thines, K. Landfester and F. R. Wurm, *RSC Adv.*, 2014, **4**, 11661–11663.
- S. Sen, S. Patil and D. S. Argyropoulos, *Green Chem.*, 2015, **17**, 4862–4887.
- W. Yang, E. Fortunati, D. Gao, G. M. Balestra, G. Giovanale, X. He, L. Torre, J. M. Kenny and D. Puglia, *ACS Sustainable Chem. Eng.*, 2018, **6**, 3502–3514.
- E. Larrañeta, M. Imízcoz, J. X. Toh, N. J. Irwin, A. Ripolin, A. Perminova, J. Domínguez-Robles, A. Rodríguez and R. F. Donnelly, *ACS Sustainable Chem. Eng.*, 2018, **6**, 9037–9046.
- M. Yousuf, A. Mollah, P. Palta, T. R. Hess, R. K. Vempati and D. L. Cocke, *Cem. Concr. Res.*, 1995, **25**, 671–682.
- S. Tan, D. Liu, Y. Qian, J. Wang, J. Huang, C. Yi, X. Qiu and Y. Qin, *Holzforschung*, 2019, **73**, 485–491.
- A. Hasan and P. Fatehi, *Appl. Clay Sci.*, 2018, **158**, 72–82.
- S. Laurichesse and L. Avérous, *Prog. Polym. Sci.*, 2014, **39**, 1266–1290.
- A. Duval and M. Lawoko, *React. Funct. Polym.*, 2014, **85**, 78–96.
- C. Wang, S. S. Kelley and R. A. Venditti, *ChemSusChem*, 2016, **9**, 770–783.
- P. Figueiredo, K. Lintinen, J. T. Hirvonen, M. A. Kostiainen and H. A. Santos, *Prog. Mater. Sci.*, 2018, **93**, 233–269.
- D. Kai, M. J. Tan, P. L. Chee, Y. K. Chua, Y. L. Yap and X. J. Loh, *Green Chem.*, 2016, **18**, 1175–1200.
- M. S. Ganewatta, H. N. Lokupitiya and C. Tang, *Polymers*, 2019, **11**, 1176.
- T. M. Budnyak, A. Slabon and M. H. Sipponen, *ChemSusChem*, 2020, DOI: 10.1002/cssc.202000216.
- M. N. Collins, M. Nechifor, F. Tanasă, M. Zănoagă, A. McLoughlin, M. A. Strozyk, M. Culebras and C. A. Teacă, *Int. J. Biol. Macromol.*, 2019, **131**, 828–849.
- W. J. Liu, H. Jiang and H. Q. Yu, *Green Chem.*, 2015, **17**, 4888–4907.
- L. Dong, L. Lin, X. Han, X. Si, X. Liu, Y. Guo, F. Lu, S. Rudić, S. F. Parker, S. Yang and Y. Wang, *Chem*, 2019, **5**, 1521–1536.
- C. Crestini, H. Lange, M. Sette and D. S. Argyropoulos, *Green Chem.*, 2017, **19**, 4104–4121.
- S. Constant, H. L. J. Wienk, A. E. Frissen, P. De Peinder, R. Boelens, D. S. Van Es, R. J. H. Grisel, B. M. Weckhuysen, W. J. J. Huijgen, R. J. A. Gosselink and P. C. A. Bruijnincx, *Green Chem.*, 2016, **18**, 2651–2665.
- Z. Sun, B. Fridrich, A. De Santi, S. Elangovan and K. Barta, *Chem. Rev.*, 2018, **118**, 614–678.
- B. M. Upton and A. M. Kasko, *Chem. Rev.*, 2016, **116**, 2275–2306.
- S. P. S. Chundawat, G. T. Beckham, M. E. Himmel and B. E. Dale, *Annu. Rev. Chem. Biomol. Eng.*, 2011, **2**, 121–145.
- X. Pan, C. Arato, N. Gilkes, D. Gregg, W. Mabee, K. Pye, Z. Xiao, X. Zhang and J. Saddler, *Biotechnol. Bioeng.*, 2005, **90**, 473–481.
- A. M. Galleti and C. Antonetti, Separation of Cellulose Hemicellulose, and Lignin Existing Technologies and Perspectives, *Biorefinery: From Biomass to Chemicals and Fuels*, De Gruyter, 2012, pp. 101–123.
- T. Saito, J. H. Perkins, D. C. Jackson, N. E. Trammel, M. A. Hunt and A. K. Naskar, *RSC Adv.*, 2013, **3**, 21832–21840.
- T. Saito, R. H. Brown, M. A. Hunt, D. L. Pickel, J. M. Pickel, J. M. Messman, F. S. Baker, M. Keller and A. K. Naskar, *Green Chem.*, 2012, **14**, 3295–3303.
- M. Witzler, A. Alzagameem, M. Bergs, B. El Khaldi-Hansen, S. E. Klein, D. Hielscher, B. Kamm, J. Kreyenschmidt, E. Tobiasch and M. Schulze, *Molecules*, 2018, **23**, 1–22.



43 N. Niu, Z. Ma, F. He, S. Li, J. Li, S. Liu and P. Yang, *Langmuir*, 2017, **33**, 5786–5795.

44 M. Canetti and F. Bertini, *Compos. Sci. Technol.*, 2007, **67**, 3151–3157.

45 Y. Zhao, A. Tagami, G. Dobe, M. E. Lindström and O. Sevastyanova, *Polymers*, 2019, **11**, 538.

46 X. Zhang, W. Liu, W. Liu and X. Qiu, *Int. J. Biol. Macromol.*, 2020, **142**, 551–558.

47 Q. Xing, P. Buono, D. Ruch, P. Dubois, L. Wu and W. J. Wang, *ACS Sustainable Chem. Eng.*, 2019, **7**, 4147–4157.

48 L. Liu, M. Qian, P. Song, G. Huang, Y. Yu and S. Fu, *ACS Sustainable Chem. Eng.*, 2016, **4**, 2422–2431.

49 J. Zhang, E. Fleury, Y. Chen and M. A. Brook, *RSC Adv.*, 2015, **5**, 103907.

50 K. Huang, S. Ma, S. Wang, Q. Li, Z. Wu, J. Liu, R. Liu and J. Zhu, *Green Chem.*, 2019, **21**, 4964–4970.

51 A. Duval and L. Avérous, *Green Chem.*, 2020, **22**, 1671–1680.

52 K. A. Y. Koivu, H. Sadeghifar, P. A. Nousiainen, D. S. Argyropoulos and J. Sipilä, *ACS Sustainable Chem. Eng.*, 2016, **4**, 5238–5247.

53 M. Ziegłowski, S. Trosien, J. Rohrer, S. Mehlhase, S. Weber, K. Bartels, G. Siegert, T. Trellenkamp, K. Albe and M. Biesalski, *Front. Chem.*, 2019, **7**, 562.

54 R. J. Li, J. Gutierrez, Y. L. Chung, C. W. Frank, S. L. Billington and E. S. Sattely, *Green Chem.*, 2018, **20**, 1459–1466.

55 X. Zhao, Y. Zhang, L. Wei, H. Hu, Z. Huang, M. Yang, A. Huang, J. Wu and Z. Feng, *RSC Adv.*, 2017, **7**, 52382–52390.

56 M. K. R. Konduri and P. Fatehi, *ACS Sustainable Chem. Eng.*, 2015, **3**, 1172–1182.

57 G. J. Jiao, P. Peng, S. L. Sun, Z. C. Geng and D. She, *Int. J. Biol. Macromol.*, 2019, **127**, 544–554.

58 C. Gioia, G. Lo Re, M. Lawoko and L. Berglund, *J. Am. Chem. Soc.*, 2018, **140**, 4054–4061.

59 X. Liu, H. Yin, Z. Zhang, B. Diao and J. Li, *Colloids Surf., B*, 2015, **125**, 230–237.

60 Y. S. Kim and J. F. Kadla, *Biomacromolecules*, 2010, **11**, 981–988.

61 P. Olsén, M. Jawerth, M. Lawoko, M. Johansson and L. A. Berglund, *Green Chem.*, 2019, **21**, 2478–2486.

62 Y. Sun, L. Yang, X. Lu and C. He, *J. Mater. Chem. A*, 2015, **3**, 3699–3709.

63 A. L. Korich, A. B. Fleming, A. R. Walker, J. Wang, C. Tang and P. M. Iovine, *Polymer*, 2012, **53**, 87–93.

64 H. Liu and H. Chung, *ACS Sustainable Chem. Eng.*, 2017, **5**, 9160–9168.

65 Y. Zhang, J. Liao, X. Fang, F. Bai, K. Qiao and L. Wang, *ACS Sustainable Chem. Eng.*, 2017, **5**, 4276–4284.

66 P. Buono, A. Duval, L. Averous and Y. Habibi, *Polymer*, 2017, **133**, 78–88.

67 L. Yuan, Y. Zhang, Z. Wang, Y. Han and C. Tang, *ACS Sustainable Chem. Eng.*, 2019, **7**, 2593–2601.

68 H. Chung, A. Al-Khouja and N. R. Washburn, in *Green Polymer Chemistry: Biocatalysis and Materials II*, ed. H. N. Cheng, R. A. Gross and P. B. Smith, ACS Symposium Series, American Chemical Society, Washington, D. C., 2013, vol. 1144, pp. 373–391.

69 F. G. Calvo-Flores and J. A. Dobado, *ChemSusChem*, 2010, **3**, 1227–1235.

70 Y. Matsushita, *J. Wood Sci.*, 2015, **61**, 230–250.

71 H. Ma, H. Li, W. Zhao, L. Li, S. Liu, J. Long and X. Li, *Green Chem.*, 2019, **21**, 658–668.

72 Y. Liu, C. Li, W. Miao, W. Tang, D. Xue, J. Xiao, T. Zhang and C. Wang, *Green Chem.*, 2020, **22**, 33–38.

73 S. Rautiainen, D. Di Francesco, S. N. Katea, G. Westin, D. N. Tungasmita and J. S. M. Samec, *ChemSusChem*, 2019, **12**, 404–408.

74 H. Li, A. Bunrit, N. Li and F. Wang, *Chem. Soc. Rev.*, 2020, **49**, 3748–3763, DOI: 10.1039/d0cs00078g.

75 W. Schutyser, T. Renders, S. Van Den Bosch, S. F. Koelewijn, G. T. Beckham and B. F. Sels, *Chem. Soc. Rev.*, 2018, **47**, 852–908.

76 X. Huang, C. Atay, J. Zhu, S. W. L. Palstra, T. I. Korányi, M. D. Boot and E. J. M. Hensen, *ACS Sustainable Chem. Eng.*, 2017, **5**, 10864–10874.

77 J. Becker and C. Wittmann, *Biotechnol. Adv.*, 2019, **37**, 107360.

78 A. G. Pemba, M. Rostagno, T. A. Lee and S. A. Miller, *Polym. Chem.*, 2014, **5**, 3214–3221.

79 L. Mialon, A. G. Pemba and S. A. Miller, *Green Chem.*, 2010, **12**, 1704–1706.

80 M. Firdaus and M. A. R. Meier, *Eur. Polym. J.*, 2013, **49**, 156–166.

81 S. Wang, L. Shuai, B. Saha, D. G. Vlachos and T. H. Epps, *ACS Cent. Sci.*, 2018, **4**, 701–708.

82 A. L. Holmberg, J. F. Stanzione, R. P. Wool and T. H. Epps, *ACS Sustainable Chem. Eng.*, 2014, **2**, 569–573.

83 E. A. B. da Silva, M. Zabkova, J. D. Araújo, C. A. Cateto, M. F. Barreiro, M. N. Belgacem and A. E. Rodrigues, *Chem. Eng. Res. Des.*, 2009, **87**, 1276–1292.

84 L. Zhai, *Chem. Soc. Rev.*, 2013, **42**, 7148–7160.

85 A. Lendlein and O. E. C. Gould, *Nat. Rev. Mater.*, 2019, **4**, 116–133.

86 W. Chen, C. Hu, Y. Yang, J. Cui and Y. Liu, *Materials*, 2016, **9**, 184.

87 S. Rai, B. K. Singh, P. Bhartiya, A. Singh, H. Kumar, P. K. Dutta and G. K. Mehrotra, *J. Lumin.*, 2017, **190**, 492–503.

88 B. Xue, Y. Yang, Y. Sun, J. Fan, X. Li and Z. Zhang, *Int. J. Biol. Macromol.*, 2019, **122**, 954–961.

89 Y. Shi, X. Liu, M. Wang, J. Huang, X. Jiang, J. Pang, F. Xu and X. Zhang, *Int. J. Biol. Macromol.*, 2019, **128**, 537–545.

90 Z. Ding, F. Li, J. Wen, X. Wang and R. Sun, *Green Chem.*, 2018, **20**, 1383–1390.

91 B. Zhang, Y. Liu, M. Ren, W. Li, X. Zhang, R. Vajtai, P. M. Ajayan, J. M. Tour and L. Wang, *ChemSusChem*, 2019, **12**, 4202–4210.

92 M. J. Molaei, *Anal. Methods*, 2020, **12**, 1266–1287.

93 S. Zhu, Q. Meng, L. Wang, J. Zhang, Y. Song, H. Jin, K. Zhang, H. Sun, H. Wang and B. Yang, *Angew. Chem., Int. Ed.*, 2013, **52**, 3953–3957.

94 X. Zhai, P. Zhang, C. Liu, T. Bai, W. Li, L. Dai and W. Liu, *Chem. Commun.*, 2012, **48**, 7955–7957.

95 Q. Liang, W. Ma, Y. Shi, Z. Li and X. Yang, *Carbon*, 2013, **60**, 421–428.



96 X. Liu, J. Pang, F. Xu and X. Zhang, *Sci. Rep.*, 2016, **6**, 1–8.

97 J. Song, L. Zhao, Y. Wang, Y. Xue, Y. Deng, X. Zhao and Q. Li, *Nanomaterials*, 2018, **12**, 1043.

98 V. N. Mehta, S. Jha, H. Basu, R. K. Singhal and S. K. Kailasa, *Sens. Actuators, B*, 2015, **213**, 434–443.

99 X. Yang, Y. Zhuo, S. Zhu, Y. Luo, Y. Feng and Y. Dou, *Biosens. Bioelectron.*, 2014, **60**, 292–298.

100 L. Minati and A. Del Piano, *C*, 2019, **5**(4), 77.

101 S. Cailotto, E. Amadio, M. Facchin, M. Selva, E. Pontoglio, F. Rizzolio, P. Riello, G. Toffoli, A. Benedetti and A. Perosa, *ACS Med. Chem. Lett.*, 2018, **9**, 832–837.

102 K. K. Chan, C. Yang, Y. H. Chien, N. Panwar and K. T. Yong, *New J. Chem.*, 2019, **43**, 4734–4744.

103 Z. M. S. H. Khan, R. S. Rahman, J. M. Shumaila, S. Islam and M. Zulfequar, *Opt. Mater.*, 2019, **91**, 386–395.

104 V. Raveendran, A. R. Suresh Babu and N. K. Renuka, *RSC Adv.*, 2019, **9**, 12070–12077.

105 Y. Chen, X. Sun, W. Pan, G. Yu and J. Wang, *Front. Chem.*, 2020, **7**, 911.

106 N. Arumugam and J. Kim, *Mater. Lett.*, 2018, **219**, 37–40.

107 R. Wang, G. Xia, W. Zhong, L. Chen, L. Chen, Y. Wang, Y. Min and K. Li, *Green Chem.*, 2019, **21**, 3343–3352.

108 J. Ju and W. Chen, *Anal. Chem.*, 2015, **87**, 1903–1910.

109 Y. Jiang, Y. Li, Y. Li and S. Li, *Anal. Methods*, 2016, **8**, 2448–2455.

110 B. M. Cerrutti, M. L. Moraes, S. H. Pulcinelli and C. V. Santilli, *Biosens. Bioelectron.*, 2015, **71**, 420–426.

111 A. Jędrzak, T. Rębiś, Ł. Klapiszewski, J. Zdarta, G. Milczarek and T. Jesionowski, *Sens. Actuators, B*, 2018, **256**, 176–185.

112 A. Jędrzak, T. Rębiś, M. Nowicki, K. Synoradzki, R. Mrówczyński and T. Jesionowski, *Appl. Surf. Sci.*, 2018, **455**, 455–464.

113 L. Lu, B. Liu, Z. Zhao, C. Ma, P. Luo, C. Liu and G. Xie, *Biosens. Bioelectron.*, 2012, **33**, 216–221.

114 F. Kheiri, R. E. Sabzi, E. Jannatdoust, E. Shojaeeefar and H. Sedghi, *Biosens. Bioelectron.*, 2011, **26**, 4457–4463.

115 N. Gan, X. Du, Y. Cao, F. Hu, T. Li and Q. Jiang, *Materials*, 2013, **6**, 1255–1269.

116 Z. Zhang, Y. Cong, Y. Huang and X. Du, *Micromachines*, 2019, **10**, 397.

117 M. Zhou, L. Shang, B. Li, L. Huang and S. Dong, *Biosens. Bioelectron.*, 2008, **24**, 442–447.

118 E. Turkmen, S. Z. Bas, H. Gulce and S. Yıldız, *Electrochim. Acta*, 2014, **123**, 93–102.

119 M. Şenel, *Mater. Sci. Eng., C*, 2015, **48**, 287–293.

120 B. Wang, T. Shi, Y. Zhang, C. Chen, Q. Li and Y. Fan, *J. Mater. Chem. C*, 2018, **6**, 6423–6428.

121 C. Chen, X. Wang, M. Li, Y. Fan and R. Sun, *Sens. Actuators, B*, 2018, **255**, 1569–1576.

122 Q. Wang, X. Pan, C. Lin, D. Lin, Y. Ni, L. Chen, L. Huang, S. Cao and X. Ma, *Chem. Eng. J.*, 2019, **370**, 1039–1047.

123 F. A. C. Faria, D. V. Evtuguin, A. Rudnitskaya, M. T. S. R. Gomes, J. A. B. P. Oliveira, M. P. F. Graça and L. C. Costa, *Polym. Int.*, 2012, **61**, 788–794.

124 A. Rudnitskaya, D. V. Evtuguin, L. C. Costa, M. P. Pedro Graça, A. J. S. Fernandes, M. Rosario Correia, M. T. Teresa Gomes and J. A. B. P. Oliveira, *Analyst*, 2013, **138**, 501–508.

125 K. M. Zia, H. N. Bhatti and I. Ahmad Bhatti, *React. Funct. Polym.*, 2007, **67**, 675–692.

126 K. Matyjaszewski, *Macromolecules*, 2012, **45**, 4015–4039.

127 Y. Xue, W. Liang, Y. Li, Y. Wu, X. Peng, X. Qiu, J. Liu and R. Sun, *J. Agric. Food Chem.*, 2016, **64**, 9592–9600.

128 A. Moreno, G. Lligadas, J. C. Ronda, M. Galià and V. Cádiz, *Polym. Chem.*, 2019, **10**, 5215–5227.

129 H. Y. Tse, S. C. Cheng, C. S. Yeung, C. Y. Lau, W. H. Wong, C. Dong and S. Y. Leu, *Green Chem.*, 2019, **21**, 1319–1329.

130 M. H. Sipponen, H. Lange, C. Crestini, A. Henn and M. Österberg, *ChemSusChem*, 2019, **12**, 2039–2054.

131 S. Iravani and R. S. Varma, *Green Chem.*, 2020, **22**, 612–636.

132 M. Österberg, M. H. Sipponen, B. D. Mattos and O. J. Rojas, *Green Chem.*, 2020, **22**, 2712–2733.

133 Z. Ma, C. Liu, N. Niu, Z. Chen, S. Li, S. Liu and J. Li, *ACS Sustainable Chem. Eng.*, 2018, **6**, 3169–3175.

134 S. Singha, Y. W. Jun, J. Bae and K. H. Ahn, *Anal. Chem.*, 2017, **89**, 3724–3731.

135 Y. Xue, X. Qiu, Z. Liu and Y. Li, *ACS Sustainable Chem. Eng.*, 2018, **6**, 7695–7703.

136 M. Kaushik and A. Moores, *Green Chem.*, 2016, **18**, 622–637.

137 M. Rycenga, C. M. Cobley, J. Zeng, W. Li, C. H. Moran, Q. Zhang, D. Qin and Y. Xia, *Chem. Rev.*, 2011, **111**, 3669–3712.

138 N. A. Azmi, S. H. Ahmad and S. C. Low, *RSC Adv.*, 2018, **8**, 251–261.

139 G. Milczarek, T. Rebis and J. Fabianska, *Colloids Surf., B*, 2013, **105**, 335–341.

140 Z. Shen, Y. Luo, Q. Wang, X. Wang and R. Sun, *ACS Appl. Mater. Interfaces*, 2014, **6**, 16147–16155.

141 T. Leskinen, J. Witos, J. J. Valle-Delgado, K. Lintinen, M. Kostiainen, S. K. Wiedmer, M. Österberg and M. L. Mattinen, *Biomacromolecules*, 2017, **18**, 2767–2776.

142 C. Jin, W. Song, T. Liu, J. Xin, W. C. Hiscox, J. Zhang, G. Liu and Z. Kong, *ACS Sustainable Chem. Eng.*, 2018, **6**, 1763–1771.

143 A. Zerpa, L. Pakzad and P. Fatehi, *ACS Omega*, 2018, **3**, 8233–8242.

144 L. Dai, Y. Li, F. Kong, K. Liu, C. Si and Y. Ni, *ACS Sustainable Chem. Eng.*, 2019, **7**, 13497–13504.

145 Y. Wang, M. S. Shim, N. S. Levinson, H. W. Sung and Y. Xia, *Adv. Funct. Mater.*, 2014, **24**, 4206–4220.

146 S. Mura, J. Nicolas and P. Couvreur, *Nat. Mater.*, 2013, **12**, 991–1003.

147 M. Wei, Y. Gao, X. Li and M. J. Serpe, *Polym. Chem.*, 2017, **8**, 127–143.

148 B. Diao, Z. Zhang, J. Zhu and J. Li, *RSC Adv.*, 2014, **4**, 42996–43003.

149 Y. Qian, Q. Zhang, X. Qiu and S. Zhu, *Green Chem.*, 2014, **16**, 4963–4968.

150 P. Figueiredo, C. Ferro, M. Kemell, Z. Liu, A. Kiriazis, K. Lintinen, H. F. Florindo, J. Yli-Kauhaluoma, J. Hirvonen, M. A. Kostiainen and H. A. Santos, *Nanomedicine*, 2017, **12**, 2581–2596.

151 M. H. Sipponen, H. Lange, M. Ago and C. Crestini, *ACS Sustainable Chem. Eng.*, 2018, **6**, 9342–9351.



152 M. S. Alqahtani, A. Alqahtani, A. Al-Thabit, M. Roni and R. Syed, *J. Mater. Chem. B*, 2019, **7**, 4461–4473.

153 N. Chen, L. A. Dempere and Z. Tong, *ACS Sustainable Chem. Eng.*, 2016, **4**, 5204–5211.

154 J. Zhao, D. Zheng, Y. Tao, Y. Li, L. Wang, J. Liu, J. He and J. Lei, *Biochem. Eng. J.*, 2020, **156**, 107526.

155 M. Pishnamazi, H. Hafizi, S. Shirazian, M. Culebras, G. M. Walker and M. N. Collins, *Polymers*, 2019, **11**, 1059.

156 L. Cheng, B. Deng, W. Luo, S. Nie, X. Liu, Y. Yin, S. Liu, Z. Wu, P. Zhan, L. Zhang and J. Chen, *J. Agric. Food Chem.*, 2020, **68**, 5249–5258.

157 T. P. Li, W. P. Wong, L. C. Chen, C. Y. Su, L. G. Chen, D. Z. Liu, H. O. Ho and M. T. Sheu, *Sci. Rep.*, 2017, **7**, 1–10.

158 K. E. Washington, R. N. Kularatne, M. C. Biewer and M. C. Stefan, *ACS Biomater. Sci. Eng.*, 2018, **4**, 997–1004.

159 R. Peng, D. Yang, X. Qiu, Y. Qin and M. Zhou, *Int. J. Biol. Macromol.*, 2020, **151**, 421–427.

160 G. Kocak, C. Tuncer and V. Bütün, *Polym. Chem.*, 2017, **8**, 144–176.

161 L. Liu, L. Rui, Y. Gao and W. Zhang, *Polym. Chem.*, 2015, **6**, 1817–1829.

162 J. Hu, M. R. Whittaker, Y. Li, J. F. Quinn and T. P. Davis, *Polym. Chem.*, 2015, **6**, 2407–2415.

163 P. Bilalis, D. Skoulas, A. Karatzas, J. Marakis, A. Stamogiannos, C. Tsimblouli, E. Sereti, E. Stratikos, K. Dimas, D. Vlassopoulos and H. Iatrou, *Biomacromolecules*, 2018, **19**, 3840–3852.

164 A. Moreno, J. C. Ronda, V. Cádiz, M. Galià, G. Lligadas and V. Percec, *Biomacromolecules*, 2019, **20**, 3200–3210.

165 P. Schattling, F. D. Jochum and P. Theato, *Polym. Chem.*, 2014, **5**, 25–36.

166 J. Zhuang, M. R. Gordon, J. Ventura, L. Li and S. Thayumanavan, *Chem. Soc. Rev.*, 2013, **42**, 7421–7435.

167 M. Lievonen, J. J. Valle-Delgado, M. L. Mattinen, E. L. Hult, K. Lintinen, M. A. Kostiainen, A. Paananen, G. R. Szilvay, H. Setälä and M. Österberg, *Green Chem.*, 2016, **18**, 1416–1422.

168 D. Piccinino, E. Capecchi, L. Botta, P. Bollella, R. Antiochia, M. Crucianelli and R. Saladino, *Catal. Sci. Technol.*, 2019, **9**, 4125–4134.

169 T. Zou, M. H. Sipponen and M. Österberg, *Front. Chem.*, 2019, **7**, 320.

170 M. H. Sipponen, M. Smyth, T. Leskinen, L. S. Johansson and M. Österberg, *Green Chem.*, 2017, **19**, 5831–5840.

171 M. H. Sipponen, M. Farooq, J. Koivisto, A. Pellis, J. Seitsonen and M. Österberg, *Nat. Commun.*, 2018, **9**, 2300.

172 E. Capecchi, D. Piccinino, B. M. Bizzarri, D. Avitabile, C. Pelosi, C. Colantonio, G. Calabro and R. Saladino, *Biomacromolecules*, 2019, **20**, 1975–1988.

173 J. Ou, K. Liu, J. Jiang, D. A. Wilson, L. Liu, F. Wang, S. Wang, Y. Tu and F. Peng, *Small*, 2020, **1906184**, 1–16.

174 I. Ortiz-Rivera, M. Mathesh and D. A. Wilson, *Acc. Chem. Res.*, 2018, **51**, 1891–1900.

175 Q. Feng, F. Chen and H. Wu, *BioResources*, 2011, **6**, 4942–4952.

176 D. Kai, Z. W. Low, S. S. Liow, A. Abdul Karim, H. Ye, G. Jin, K. Li and X. J. Loh, *ACS Sustainable Chem. Eng.*, 2015, **3**, 2160–2169.

177 *Lignin and Lignans Advances in Chemistry*, ed. C. Heitner, D. R. Dimmel and J. A. Schmidt, CRC Press, New York, 2010.

178 *Chemical Modification, Properties and Usage of Lignin*, ed. T. Q. Hu, Kluwer Academic/Plenum, New York, 2002.

179 K. Lintinen, Y. Xiao, R. Bangalore Ashok, T. Leskinen, E. Sakarinen, M. Sipponen, F. Muhammad, P. Oinas, M. Österberg and M. Kostiainen, *Green Chem.*, 2018, **20**, 843–850.

180 M. Farooq, T. Zou, G. Riviere, M. H. Sipponen and M. Österberg, *Biomacromolecules*, 2019, **20**, 693–704.

181 H. Li, Y. Deng, B. Liu, Y. Ren, J. Liang, Y. Qian, X. Qiu, C. Li and D. Zheng, *ACS Sustainable Chem. Eng.*, 2016, **4**, 1946–1953.

182 D. Tian, J. Hu, J. Bao, R. P. Chandra, J. N. Saddler and C. Lu, *Biotechnol. Biofuels*, 2017, **10**, 1–11.

183 N. Bensabeh, A. Moreno, A. Roig, M. Rahimzadeh, K. Rahimi, J. C. Ronda, V. Cádiz, M. Galià, V. Percec, C. Rodriguez-Emmenegger and G. Lligadas, *ACS Sustainable Chem. Eng.*, 2020, **8**, 1276–1284.

184 R. Hilgers, G. Van Erven, V. Boerkamp, I. Sulaeva, A. Potthast, M. A. Kabel and J. P. Vincken, *Green Chem.*, 2020, **22**, 1735–1746.

185 A. Lendlein and S. Kelch, *Angew. Chem., Int. Ed.*, 2002, **41**, 2034–2057.

186 A. Lendlein, H. Jiang, O. Jünger and R. Langer, *Nature*, 2005, **434**, 879–882.

187 Y. Wang, W. Tian, J. Xie and Y. Liu, *Micromachines*, 2016, **8**, 145.

188 J. Mendez, P. K. Annamalai, S. J. Eichhorn, R. Rusli, S. J. Rowan, E. J. Foster and C. Weder, *Macromolecules*, 2011, **44**, 6827–6835.

189 R. Mohr, K. Kratz, T. Weigel, M. Lucka-Gabor, M. Moneke and A. Lendlein, *Proc. Natl. Acad. Sci. U. S. A.*, 2006, **103**, 3540–3545.

190 E. Smela, *Adv. Mater.*, 2003, **15**, 481–494.

191 W. Small IV, P. Singhal, T. S. Wilson and D. J. Maitland, *J. Mater. Chem.*, 2010, **20**, 3356–3366.

192 Q. Shi, H. Liu, D. Tang, Y. Li, X. J. Li and F. Xu, *NPG Asia Mater.*, 2019, **11**, 64.

193 Y. Xu, K. Odelius and M. Hakkainen, *ACS Sustainable Chem. Eng.*, 2019, **7**, 13456–13463.

194 P. Mora, H. Schäfer, C. Jubsilp, S. Rimdusit and K. Koschek, *Chem. – Asian J.*, 2019, **14**, 4129–4139.

195 G. M. Scheutz, J. J. Lessard, M. B. Sims and B. S. Sumerlin, *J. Am. Chem. Soc.*, 2019, **141**, 16181–16196.

196 J. J. Lessard, G. M. Scheutz, S. H. Sung, K. A. Lantz, T. H. Epps and B. S. Sumerlin, *J. Am. Chem. Soc.*, 2020, **142**, 283–289.

197 B. Hendriks, J. Waelkens, J. M. Winne and F. E. Du Prez, *ACS Macro Lett.*, 2017, **6**, 930–934.

198 F. Gamardella, F. Guerrero, S. De la Flor, X. Ramis and A. Serra, *Eur. Polym. J.*, 2020, **122**, 109361.

199 S. Zhang, T. Liu, C. Hao, L. Wang, J. Han, H. Liu and J. Zhang, *Green Chem.*, 2018, **20**, 2995–3000.

200 C. Borsellino, G. Di Bella and V. F. Ruisi, *Int. J. Adhes. Adhes.*, 2009, **29**, 36–44.

201 S. G. Prolongo, G. Del Rosario and A. Ureña, *Int. J. Adhes. Adhes.*, 2006, **26**, 125–132.



202 F. Gamardella, S. De la Flor, X. Ramis and A. Serra, *React. Funct. Polym.*, 2020, **151**, 104574.

203 H. Li, G. Sivasankarapillai and A. G. McDonald, *Ind. Crops Prod.*, 2015, **67**, 143–154.

204 G. Sivasankarapillai, H. Li and A. G. McDonald, *Biomacromolecules*, 2015, **16**, 2735–2742.

205 H. Liu, N. Mohsin, S. Kim and H. Chung, *J. Polym. Sci., Part A: Polym. Chem.*, 2019, **57**, 2121–2130.

206 N. A. Nguyen, K. M. Meek, C. C. Bowland, S. H. Barnes and A. K. Naskar, *Macromolecules*, 2018, **51**, 115–127.

207 N. A. Nguyen, K. M. Meek, C. C. Bowland and A. K. Naskar, *Polymer*, 2019, **160**, 210–222.

208 J. Huang, W. Liu and X. Qiu, *ACS Sustainable Chem. Eng.*, 2019, **7**, 6550–6560.

209 Y. Bai, X. Zhang, Q. Wang and T. Wang, *J. Mater. Chem. A*, 2014, **2**, 4771–4778.

210 Z. Ding, L. Yuan, T. Huang, G. Liang and A. Gu, *Ind. Eng. Chem. Res.*, 2019, **58**, 8734–8742.

211 J. Liu, S. Wang, Z. Tang, J. Huang, B. Guo and G. Huang, *Macromolecules*, 2016, **49**, 8593–8604.

212 L. Xue, S. Dai and Z. Li, *Biomaterials*, 2010, **31**, 8132–8140.

213 R. Dhanasekaran, S. Sreenatha Reddy, B. Girish Kumar and A. S. Anirudh, *Mater. Today Proc.*, 2018, **5**, 21427–21435.

214 R. Liu, X. Kuang, J. Deng, Y. C. Wang, A. C. Wang, W. Ding, Y. C. Lai, J. Chen, P. Wang, Z. Lin, H. J. Qi, B. Sun and Z. L. Wang, *Adv. Mater.*, 2018, **30**, 1–8.

215 M. Fasihi and H. Mansouri, *J. Appl. Polym. Sci.*, 2016, **133**, 44068.

216 A.-V. Ruzette and L. Leibler, *Nat. Mater.*, 2005, **4**, 19–31.

217 K. Kumar, C. Knie, D. Bléger, M. A. Peletier, H. Friedrich, S. Hecht, D. J. Broer, M. G. Debije and A. P. H. J. Schenning, *Nat. Commun.*, 2016, **7**, 11976.

218 M. Yamada, M. Kondo, J. I. Mamiya, Y. Yu, M. Kinoshita, C. J. Barrett and T. Ikeda, *Angew. Chem., Int. Ed.*, 2008, **47**, 4986–4988.

219 L. Dai, M. Ma, J. Xu, C. Si, X. Wang, Z. Liu and Y. Ni, *Chem. Mater.*, 2020, **32**, 4324–4330.

220 G. Yilmaz and C. R. Becer, *Polym. Chem.*, 2015, **6**, 5503–5514.

221 O. Cusola, O. J. Rojas and M. B. Roncero, *ACS Appl. Mater. Interfaces*, 2019, **11**, 45226–45236.

222 A. X. Lu, H. Oh, J. L. Terrell, W. E. Bentley and S. R. Raghavan, *Chem. Sci.*, 2017, **8**, 6893–6903.

223 Y. Huang, L. Deng, P. Ju, L. Huang, H. Qian, D. Zhang, X. Li, H. A. Terryn and J. M. C. Mol, *ACS Appl. Mater. Interfaces*, 2018, **10**, 23369–23379.

224 M. Wang, Y. Zhai, H. Ye, Q. Lv, B. Sun, C. Luo, Q. Jiang, H. Zhang, Y. Xu, Y. Jing, L. Huang, J. Sun and Z. He, *ACS Nano*, 2019, **13**, 7010–7023.

225 X. Liu, P. Formanek, B. Voit and D. Appelhans, *Angew. Chem., Int. Ed.*, 2017, **56**, 16233–16238.

226 P. Schattling, F. D. Jochum and P. Theato, *Chem. Commun.*, 2011, **47**, 8859–8861.

